Auxin methylation during establishment and evolution of root nodule symbiosis

（根粒共生の成立過程と進化におけるオーキシンメチル化）

Goto, Takashi

後藤　崇支

The Graduate University for Advanced Studies, SOKENDAI

School of Life Science

Department of Basic Biology

2023

TABLE OF CONTENTS

Chapter 1 GENERAL INTRODUCTION

Symbiosis is a strategy for living organisms to overcome challenges that alone would be difficult. For plants, nitrogen nutrition is essential for growth. Leguminous plants adapt to nitrogen-poor soils, by recruiting nitrogen-fixing bacteria into their roots and accommodating them in de novo symbiotic organs called root nodules. The root nodule symbiosis is found in plant families belonging to the nitrogen-fixing clade, a monophyletic group, which consists of four orders: Fagales, Cucurbitales, Rosales, and Fabales (Soltis et al. 1995) (Fig. 1). Fabaceae (legume) family and non-legume genus *Parasponia*, possesses rhizobia as symbiotic partners. Among Fagales, Cucurbitales, Rosales with the exception of *Parasponia,* those that engage in nodule symbiosis are referred to as actinorhizal plants, with *Frankia* generally known as symbiotic bacteria (Benson and Silvester 1993) (Fig. 1).

A predisposition for root nodule symbiosis is estimated to have acquired in the common ancestor of the four orders more than 100 million years ago (Soltis et al. 1995; Werner et al. 2014) (Fig. 1). However, root nodule symbiosis is found in only 10 of the 28 families in the four orders (Doyle 2011) (Fig. 1). Moreover, most genera in nine of these 10 families does not form root nodule symbiosis, whereas most legume maintains root nodule symbiosis (Doyle 2011). Phylogenomics in the nitrogen-fixing clades was conducted to follow these questions, and suggests that at least eight independent losses of nodule symbioses have occurred (Griesmann et al. 2018). Therefore, the scattered distribution of root nodule symbiosis within the nitrogen-fixing clades can be explained by independent losses after acquisition of root nodule symbiosis. On the other hand, it remains unclear how most legumes retain root nodule symbiosis compared to species of

other families, and legumes appear to have somehow established an evolutionarily robust symbiotic system. The phylogenomics also provides a clue of that: OrthoFinder (Emms and Kelly 2015) did not detect any novel genes associated with evolution of the nitrogen-fixing clade (Griesmann et al. 2018), which indicates possible co-options of existing gene and rearrangement of signaling pathways during evolution in the nitrogen-fixing clade.

In general, the process of nodule formation of legumes consists of rhizobial infection in root epidermis and subsequent primordium formation that occurs in the underlying layer. Here it is described as to the regulatory system based on the findings obtained through the model legume, *Lotus japonicus* (Fig. 2A). In epidermis, lipochitin oligosaccharide (Nod factor) produced by rhizobia is recognized by the receptors on root-hair cells of host plants (Broghammer et al. 2012; Madsen et al. 2003; Radutoiu et al. 2003). This allows the deformation and curling of root-hairs and the formation of infection threads (ITs), plant-derived intracellular tubular structures. After being trapped by the curling root hairs, rhizobia are taken up through ITs from epidermis into cortex. The formation of nodule primordium is initiated by cortical cell division below the infection site in epidermis. Rhizobia then invade the dividing cortical cells. Here, epidermal infection and developmental program in cortex need to be spatiotemporally coordinated by host plant. However, how this spatiotemporal synchronization is achieved remains little understood. In addition, another important question is how, while epidermal infection system has been developed especially in the legume lineages among the nitrogen-fixing clade, this system could have been evolutionarily combined with the developmental system acquired in the nitrogen-fixing clade.

Regarding the molecular mechanisms involved in the epidermal infection, calcium influx occurs in response to Nod factor in root-hair cells, and periodic calcium

oscillations in nucleus are triggered by CASTOR/POLLUX (Imaizumi-Anraku et al. 2005; Sieberer et al. 2009). The oscillations are decoded by calcium/calmodulin-dependent protein kinase (CCaMK) (Lévy et al. 2004; Tirichine et al. 2006). CYCLOPS, a phosphorylation target of CCaMK, activates expression of key transcription factors that govern downstream responses leading to infection (Cerri et al. 2017; Singh et al. 2014; Yano et al. 2008) (Fig. 2B). For example, *ERF REQUIRED FOR NODULATION 1* (*ERN1*), whose promoter is a binding target of CYCLOPS (Cerri et al. 2017), is required for root-hair deformation and subsequent IT formation (Cerri et al. 2012, 2017; Kawaharada et al. 2017; Middleton et al. 2007; Yano et al. 2017). *ern1* mutant reduced auxin accumulation (Nadzieja et al. 2018), and auxin biosynthesis and signaling in epidermis are required for epidermal infection (Breakspear et al. 2014; Nadzieja et al. 2018).

A transcription factor NODULE INCEPTION (NIN) plays a central role in the cortical cell division. *NIN* is expressed in both epidermis and cortex and is required for both IT formation in epidermis and cell division in cortex. *nin* mutant is defective in IT and primordium formation, and constitutive expression of *NIN* induces cortical cell division (Schauser et al. 1999; Soyano et al. 2013). The *NIN* promoter contains a CYCLOPS binding site, a gibberellin response element, and cytokinin response elements, which are located at 0.7 kb upstream (Singh et al. 2014), 1.2 kb upstream (Akamatsu et al. 2021), and 15 kb ~ 20 kb upstream (Liu et al. 2019), respectively in *L. japonicus*. The spatial expression and function of *NIN* can be explained by usage of these cis-regulatory regions: the CYCLOPS binding site is important for IT formation (Akamatsu, Nagae, and Takeda 2022), and symbiotic mutants *daphne* (in *L. japonicus*) or *daphne-like* (*in Medicago truncatula*), lacking the upstream of >7 kb or >4 kb, respectively, display

epidermal ITs but does not produce nodule primordium in cortex (Liu et al. 2019; Yoro et al. 2014). Application of cytokinin to *L. japonicus* roots induces *NIN* expression and bump formation (Heckmann et al. 2011), and a gain-of-function mutant of a cytokinin receptor spontaneously produces nodule-like structures (Tirichine et al. 2007). For gibberellins, its application to legume roots can induce cell division in pericycle (Kawaguchi et al. 1996), and also induces *NIN* expression (Akamatsu et al. 2021).

Regarding the mechanisms involved in the coordination of epidermal infection and cortical development, regulation of callose turnover in plasmodesmata (channel-like structures that connect neighboring cells and allow cell-to-cell molecular transport in plant) is involved (Gaudioso-Pedraza et al. 2018). Induction of callose synthesis suppresses *NIN* expression in cortex, highlighting the importance of intercellular communication in the nodulation process. Interestingly, epidermis-specific expression of early symbiotic genes such as CASTOR/POLLUX is sufficient for nodule formation in cortex in their corresponding mutants (Hayashi et al. 2014), suggesting that unknown signals from infected epidermis would induce cortical cell division. Therefore, identification of the signaling across root tissues during the symbiotic process is important for understanding the spatiotemporal synchronization of epidermal infection and cortical development.

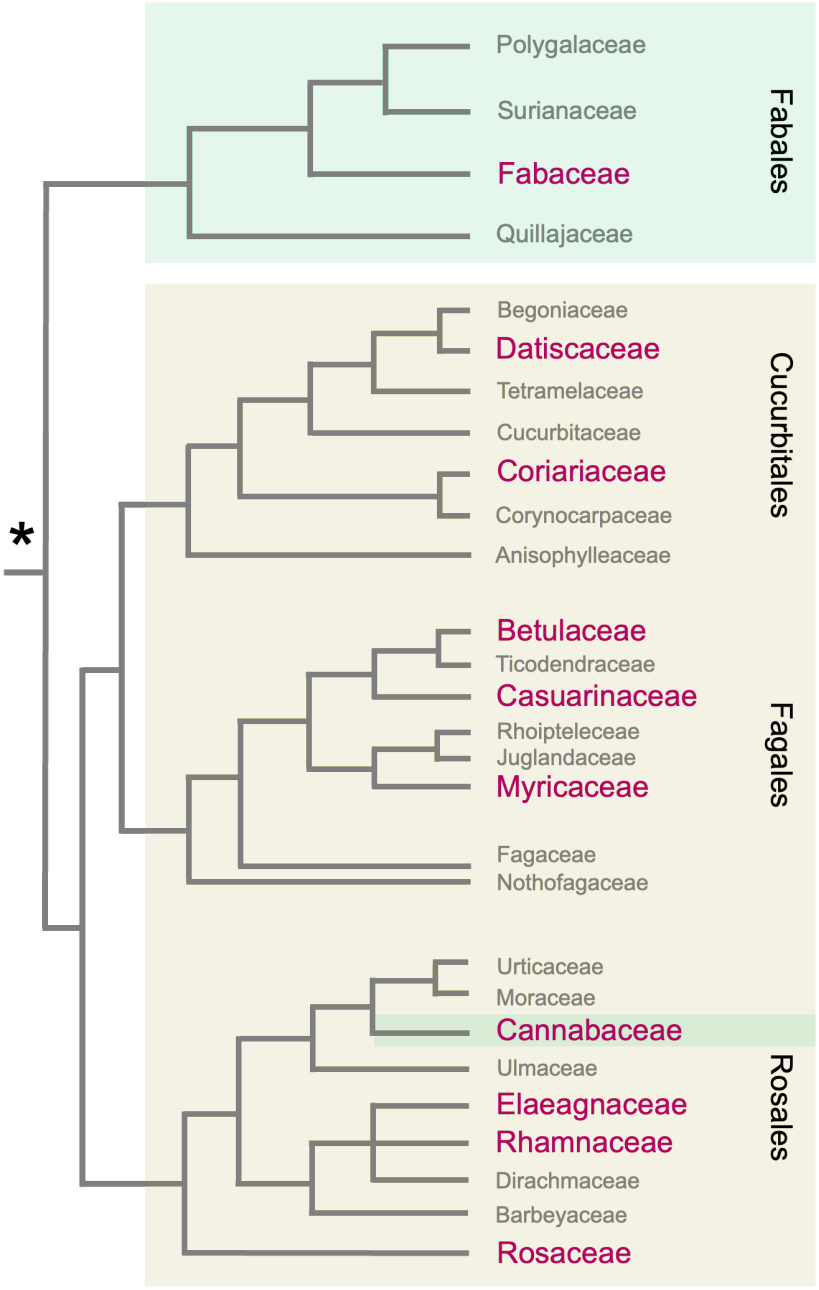

Figure 1. The nitrogen-fixing clade and Nodule symbiosis. Nodule symbiosis is observed in the nitrogen-fixing clade, which consists of four orders. Fabaceae and *Parasponia* (Cannabaceae) have rhizobia as symbiotic partners (green boxes). Among Fagales, Cucurbitales, Rosales, some have nodule symbiosis with *Frankia* (a brown box). Nodule symbiosis is observed only in the 10 families marked in pink. An asterisk indicates a presumed predisposition that led to the later acquisition of nodule symbiosis.

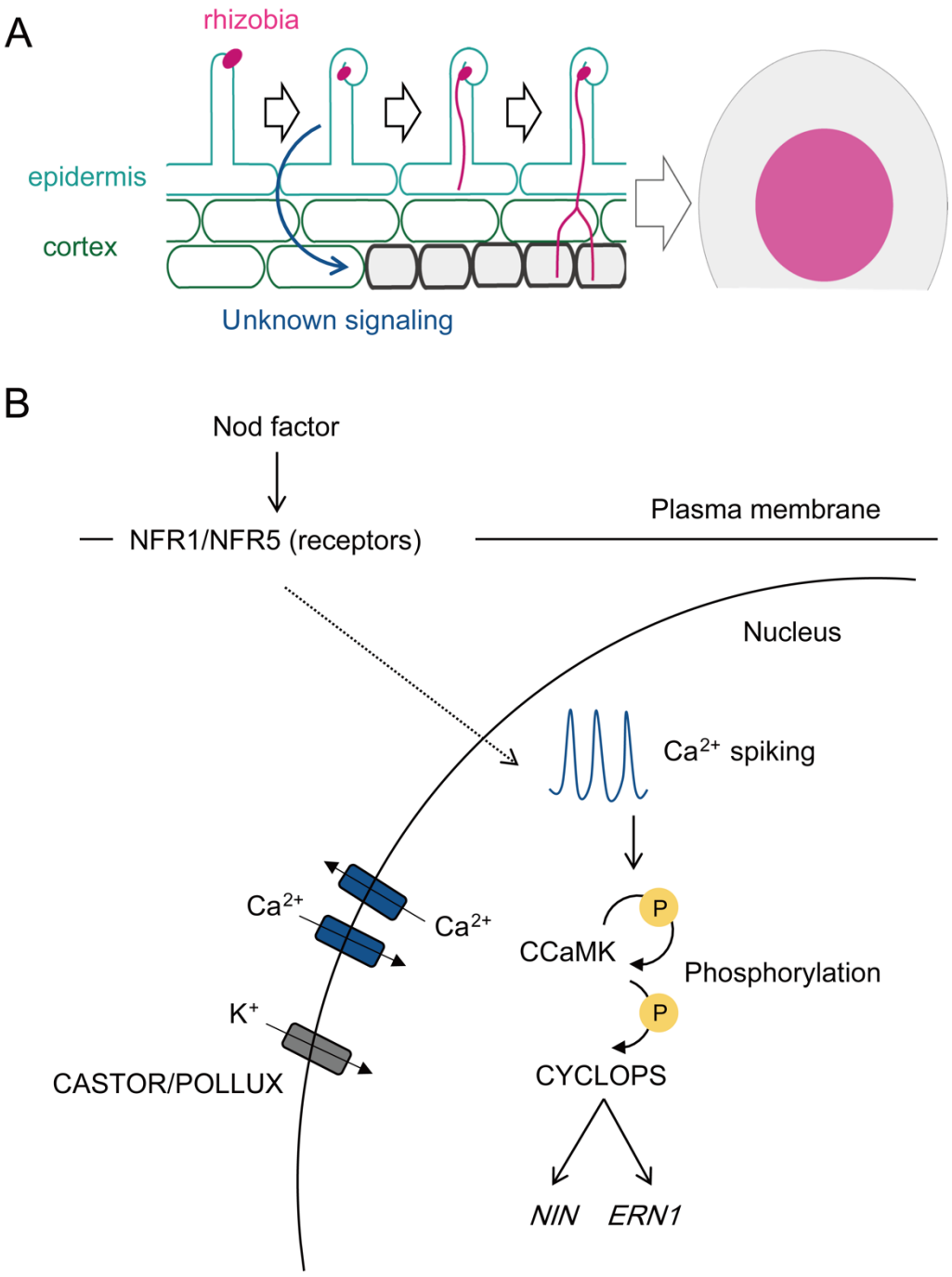

Figure 2. Schematic illustration of nodulation process (A) and signaling (B).

(A) Nodule formation consists of two biological events: rhizobial infection in root epidermis, and subsequent nodule formation with cell division in root cortex. Rhizobia (pink oval) are trapped by deformed root-hairs, and then taken up from epidermis into cortex through infection threads (IT; pink line). Cortical cell division occurs just below

the infected epidermis, and provides an indispensable scaffold for IT progression from epidermis to cortex. In this context, some kind of unknown signal, generated in the infected epidermis, trigger cortical cell division (blue arrow). **(B)** Nod factor produced by rhizobia is recognized by its receptors NFR1/5 at plasma membrane. CASTOR/POLLUX is involved in Ca2+ spiking at nucleus. The Ca^{2+} spiking is decoded by CCaMK, which is subsequently autophosphorylated and phosphorylates CYCLOPS. CYCLOPS orchestrates gene expression of symbiotic transcription factors, such as NIN and ERN1.

Chapter 2 Auxin methylation by *IAMT1*, duplicated in the legume lineage, promotes root nodule development in *Lotus japonicus*

2.1 Introduction

Legumes develop de novo organs known as root nodules to accommodate symbiotic bacteria called rhizobia. Nodule formation involves two distinct processes: rhizobial infection involving host-microbe communication via signaling molecules in root epidermis, and nodule primordium development accompanied by cell division in root cortex. In epidermis, rhizobia-derived lipochitin oligosaccharide (Nod factor) binds to LysM receptor-like kinases (NFR1/5) in host root-hair cells (Broghammer et al. 2012; Madsen et al. 2003; Radutoiu et al. 2003). This triggers periodic calcium spiking, which is decoded by CCaMK (Ehrhardt, Wais, and Long 1996; Lévy et al. 2004; Sieberer et al. 2009; Tirichine et al. 2006). CYCLOPS, a direct phosphorylation substrate of CCaMK, acts as a transcription activator of *NIN* and *ERN1* (Cerri et al. 2017; Marsh et al. 2007; Singh et al. 2014; Yano et al. 2008), which are necessary to form microcolonies in infection chambers and infection threads (ITs) (Fournier et al. 2015; Kawaharada et al. 2017; Middleton et al. 2007; Schauser et al. 1999; Yano et al. 2017).

Cortical cell division, which occurs just below the site of rhizobial infection in epidermis, is required for primordium development. Phytohormones are important for cortical cell division. Exogenous cytokinin application induces ectopic cortical cell division (Heckmann et al. 2011). Some cytokinin receptor genes, such as *Lotus histidine kinase* (*LHK*), are induced in dividing cortical cells upon rhizobial infection (Held et al. 2014). Gain-of-function LHK1 causes spontaneous nodulation (Tirichine et al. 2007).

Loss-of-function or knockdown of *LHK1* or the homologous gene, *Medicago truncatula CRE1*, inhibits nodulation (Gonzalez-Rizzo, Crespi, and Frugier 2006; Murray et al. 2007). Cortical cell division also provides an indispensable scaffold for IT progression from epidermis to cortex (Suzaki et al. 2014), and rhizobia are released from intracellular ITs ramified in nodule primordia, leading to successful nodule organogenesis. Recently, it has been reported that symplastic communication by callose turnover at plasmodesmata is important for coordinating epidermal infection and nodule development (Gaudioso-Pedraza et al. 2018). These findings suggest that spatiotemporal coordination across epidermis and cortex is essential for this symbiotic organogenesis. Epidermal expression of genes required for calcium spiking, such as C*ASTOR* and *POLLUX* (*DOES NOT MAKE INFECTIONS1* (*DMI1*) in *Medicago*) (Ané et al. 2004; Imaizumi-Anraku et al. 2005), *NUP85* (Saito et al. 2007), and *NUP133* (Kanamori et al. 2006), is sufficient for nodule formation (Hayashi et al. 2014), suggesting that some kind of signals generated in epidermis trigger cortical cell division. However, little is known about the mechanism that coordinates these two events.

Among various symbiotic mutants of *L. japonicus*, *daphne* is an intriguing non-nodulation mutant in which epidermal infection is uncoupled from cortical cell division (Yoro et al. 2014). In *daphne*, excess ITs are formed in the epidermis, but cortical cell division is not activated. The *daphne* mutation is a chromosome translocation 7 kb upstream of the *NIN* start codon, resulting in a lack of *NIN* expression in cortex, but not in epidermis. *NIN* expression is involved in both epidermal IT formation and initiation of cortical cell division (Marsh et al. 2007; Schauser et al. 1999; Soyano et al. 2013), and the regulatory nucleotide sequences for *NIN* expression differ between root tissues (Liu et al. 2019; Yoro et al. 2014). CYC-box, the CYCLOPS binding site, in the *NIN* promoter

is sufficient for IT formation. CE, Cytokinin response element, in the *NIN* promoter is required for nodule formation in *Medicago* (Liu et al. 2019). Cortical *NIN* not only induces cortical cell division, but also represses excessive infection in epidermis, and a lack of cortical *NIN* expression causes the *daphne* phenotype (Yoro et al. 2014). Therefore, in *daphne*, signals derived from infection in epidermis should be overproduced, and signals after cortical *NIN*-derived cell division should be reduced. On the other hand, signals that are not reflected in the *daphne* phenotype, including those that induce cortical cell division upstream or independent of cortical *NIN* and derived from epidermal infection, may be overproduced in *daphne*. Therefore, use of *daphne* to explore transcriptional profiles may allow me to uncover genes and factors that coordinate these two events, in addition to the molecular mechanisms of epidermal infection and cortical cell division.

Here, I conducted a time-course transcriptome analysis of *daphne*, and identified genes that showed different expression patterns in *daphne* and wild type (WT). Among these genes, I found *IAA CARBOXYL METHYLTRANSFERASE 1 (IAMT1)*, which encodes the enzyme that specifically converts auxin (indole acetic acid, IAA) into methyl-IAA (MeIAA) (D'Auria, Chen, and Pichersky 2003; Takubo et al. 2020; Zubieta et al. 2003). *IAMT1* is essential for shoot development and differential growth in *Arabidopsis thaliana*, a non-symbiotic plant (Abbas et al. 2018; Qin et al. 2005), but as far as I know, there have been no reports on detailed expression and function analysis of *IAMT1* in roots. In this study, I found that *IAMT1* is duplicated in the legume lineage, and one of the duplicates (named *IAMT1a*) is mainly expressed in epidermis, whereas reverse genetic analysis showed that *IAMT1a* is crucial for nodule development, rather than for epidermal infection. A significant MeIAA increase after rhizobial infection was detected by using

daphne roots. Furthermore, expression of *NIN* in WT roots increased after MeIAA treatment, in contrast to IAA treatment. Based on these findings, herein I discuss how MeIAA properties differ from those of IAA and how MeIAA may be a signaling molecule that links different events in epidermis and cortex.

2.2 Results

Time-course transcriptome analysis of *L. japonicus* MG-20 and *daphne*.

I performed time-course RNA sequencing on *L. japonicus* WT MG-20 and *daphne* at early time points after rhizobial inoculation. I set 4 time-points (0 Days After Inoculation [DAI] (non-inoculation), 1, 2, and 3 DAI.): At 1 and 2 DAI, root hair deformation and microcolony entrapment were observed. At 3 DAI, infection threads (ITs) were observed in root epidermis and cortical cell division occurred in WT, while no cortical cell division was observed in *daphne*, despite excessive IT formation.

To identify significant differentially expressed genes (DEGs) for time-course, maSigPro (Nueda, Tarazona, and Conesa 2014) was used. The time-course differential expression patterns were extracted by comparing the patterns in WT with those in *daphne*. Using a false discovery rate < 0.05 as a cut-off, 4,871 genes were classified as time-course DEGs. Hierarchical clustering of time-course DEGs that changed >2-fold (1,076 genes) revealed four subgroups, based upon expression patterns (Fig. 3A): In Cluster I (473 genes), transcript levels increased at 1 DAI in WT, but increased to a greater extent and more persistently in *daphne* (Fig. 3B). In Cluster II (204 genes), transcription was activated at 1 DAI in *daphne*, whereas in WT, transcription was unchanged or attenuated (Fig. 3B). Cluster III included 222 genes that were more highly up-regulated in WT than

daphne (Fig. 3B). Cluster IV grouped 177 genes that displayed temporal up-regulation in WT, but for which expression was not altered in *daphne* (Fig. 3B). For example, genes associated with infection events in epidermis, such as genes involved in IT formation and/or that act from infected epidermis to cortex, may be included in Clusters I and III, which show increased expression in WT. In addition, genes associated with excessive infection in *daphne* are most likely to be included in Cluster I. On the contrary, genes that positively regulate nodule primordium formation and/or act repressively from cortex to epidermal infection can be included in Cluster IV, where no induction of expression occurs in *daphne*.

Phylogenetic analysis and expression of *L. japonicus indole-3-acetic acid carboxyl methyltransferase 1*

Lj2g3v3222870 was one of the most differentially expressed DEGs in Cluster I ($p = 3.97 * 10^{-97}$). A phylogenetic tree showed that Lj2g3v3222870 is included in the IAMT1 (Indole-3-acetic acid carboxyl methyltransferase 1) clade of the SABATH family, which comprises a group of small-molecule methyltransferases (Fig. 4B). *IAMT1* encodes an enzyme that specifically converts IAA into its methyl ester (D'Auria et al. 2003; Takubo et al. 2020; Zubieta et al. 2003) (Fig. 4A), and unlike other SABATHs, it has an amino acid substitution (Trp-256 to Gly-256 in AtIAMT1) that is required for recognition and binding of the IAA indole ring (Zhao et al. 2008; Zubieta et al. 2003). This amino acid substitution was also confirmed in Lj2g3v3222870 (Fig. 5). Based on this feature and its phylogenetic relationship, I conclude that Lj2g3v3222870 is an ortholog of *A. thaliana* IAMT1. A BLASTP search identified another *IAMT1* gene (*Lj6g3v0819010*) in *L. japonicus*; hence, the two *LjIAMT1* genes (*Lj2g3v3222870* and *Lj6g3v0819010*) were

named *LjIAMT1a* and *LjIAMT1b* respectively. An analysis of a phylogenetic tree of IAMT1 proteins from various plant species suggested that the gene duplication of *IAMT1* occurred in the common ancestor of legumes (Fig. 4C).

Although both LjIAMT1a and LjIAMT1b share highly a conserved sequence containing the amino acid substitution characteristic of IAMT1 (Fig. 5), *IAMT1a* but not *IAMT1b* was differentially expressed in time-course RNA-seq as well as quantitative reverse transcription polymerase chain reaction (qRT-PCR) (Fig. 4D, 6, and 7). Despite highly conserved similarity in the legume lineage, the mRNA abundance of *IAMT1a* in roots estimated from RNA-seq data was approximately 100 times higher than that of *IAMT1b* (Fig. 4D).

IAMT1a expression pattern in the early infection stage

To determine the genetic dependency of transcriptional changes in *IAMT1a*, we conducted time-course qRT-PCR experiments on a series of symbiotic mutants after rhizobial infection. In a *nin* null mutant (*nin-9*), as well as in *daphne*, *IAMT1a* was induced more highly and continuously than in WT (Fig. 6). This indicates that *NIN* is at least unnecessary for induction of *IAMT1a* expression. In contrast, *IAMT1a* was not induced in *ccamk-14* or *ern1-6* (Fig. 6), indicating that *IAMT1a* is induced downstream of *CCaMK* and *ERN1* on the symbiotic pathway.

To identify the expression site of *IAMT1a* during early rhizobial infection, I performed a histochemical analysis. GUS signals driven by the 2.9 kbp *IAMT1a* promoter in the WT background were detected in the rhizobia-susceptible region at 2 DAI. (Fig. 8B and 8H). Expression of *proIAMT1a:tripleYFP-nls* was observed in root epidermis of the susceptible region at the same time (Fig. 8I). However, the GUS signal was attenuated

after epidermal ITs were formed (Fig. 8C, 8D and 8J). These changes in *IAMT1a* promoter activity were consistent with transient increases in its mRNA levels in WT as detected by RNA-seq and qRT-PCR (Fig. 4D and 6). In contrast, in the *daphne* background, the susceptible window remains open (Yoro et al. 2014), and GUS signals were detected in the broader root region after inoculation (Fig. 8F and 8G). Interestingly, GUS signals were detected in the region in which epidermal IT formation was observed in *daphne* (Fig. 8K). These patterns are consistent with persistent increases in its mRNA levels in *daphne* (Fig. 4D and 6).

IAMT1a knockdown affected cortical events, but not epidermal infection

To examine involvement of *IAMT1a* in nodulation, I performed RNAi knockdown (KD) analysis of *IAMT1a* in *L. japonicus*. I prepared three constructs for knockdown that targeted different sequences (5' UTR or coding sequence). *IAMT1a* and *IAMT1b* expression levels were analyzed in roots with real-time RT-PCR, 3 weeks after inoculation. In roots transformed with RNAi constructs, *IAMT1a* transcription levels were reduced to less than half of controls ($10^{-4} < p < 10^{-2}$) (Fig. 9). Transcription levels of *IAMT1b* also tended to decrease ($0.2 < p < 0.4$) (Fig. 9). On average, *IAMT1a*-RNAi-2 reduced *IAMT1a* transcripts to 10% of control levels. *IAMT1a*-RNAi-2 was the most effective for decreasing *IAMT1a* transcripts, but *IAMT1a*-RNAi-2 had the weakest effect on reducing *IAMT1b* transcripts (Fig. 9). When the number of nodules was measured 3 weeks after inoculation, the number of nodules decreased significantly in hairy roots transformed with *IAMT1a*-RNAi vectors (Fig. 10). Nodules were not observed in 21-33% of plants with hairy roots harboring *IAMT1a*-RNAi vectors, although nodules formed in all controls (Fig. 10). *IAMT1a*-RNAi also significantly inhibited formation of nodule

primordia at 7 DAI. (Fig. 11A). Interestingly, in *IAMT1a*-RNAi hairy roots without nodules, ITs wandered in epidermis, but did not enter the cortex (Fig. 11B). This is similar to the symbiotic phenotype of *L. japonicus vag1* and *daphne* mutants (Suzaki et al. 2014; Yoro et al. 2014).

IAMT1a-RNAi seemed not to affect epidermal infection of rhizobia in WT (Fig. 11C). To further confirm this, I performed *IAMT1a*-RNAi using a *daphne* non-nodulating mutant, which has excessive ITs due to deficient negative feedback by cortical *NIN*. As a result, excessive ITs of *daphne* were kept in *IAMT1a*-RNAi hairy roots 2 weeks after inoculation without reduction (Fig. 11C). These suggested that *IAMT1a* contributes more to cortical events than to epidermal infection.

To assess *IAMT1a* function in nodule development, I performed *IAMT1a*-RNAi in the absence of rhizobia, using *spontaneous nodule formation* (*snf*) mutants such as constitutively expressing a gain-of-function CCaMK^{T265D} (*snf1-like*) (Tirichine et al. 2006; Yano et al. 2008) or a gain-of-function LHK1 cytokinin receptor (*snf2*) (Tirichine et al. 2007). *IAMT1a*-RNAi inhibited spontaneous nodulation in *snf1-like* (Fig. 12). This indicated that *IAMT1a* acts downstream of *CCaMK*, consistent with the fact that *IAMT1a* expression was not induced in the *ccamk* mutant after rhizobial inoculation (Fig. 6). On the other hand, *IAMT1a*-RNAi did not affect spontaneous bump formation in *snf2* mutant (Fig. 12). This indicates that the function of *IAMT1a* is not under control of *LHK1*-mediated cytokinin signaling in nodule development.

Overexpression of *IAMT1a* promoted nodulation in *tml-4* mutant

To investigate whether *IAMT1a* positively regulates nodule development, I overexpressed *IAMT1a*. *IAMT1a* overexpression had no effect on nodule number in WT (Fig. 13).

However, in *tml-4* mutants, which produce excessive ITs and nodules due to lack of autoregulation of nodulation (AON) (Magori et al. 2009; Takahara et al. 2013), an increased number of nodules was observed in overexpressed *IAMT1a* (Fig. 13). In addition, I confirmed the correlation between expression levels of *IAMT1a* and nodule number (Fig. 14). These results show that *IAMT1a* is a positive regulator of nodule development.

Involvement of auxin methylation in nodule development

To clarify the presence of endogenous MeIAA during nodulation, I tried to detect MeIAA before and after rhizobial infection. Identification of endogenous MeIAA is generally difficult, because the amount of MeIAA is much less than that of IAA (Abbas et al. 2018). Therefore, I used *daphne*, in which rhizobial infection and accumulation of *IAMT1a* transcripts were enhanced (Fig. 4D and 6). The use of *daphne* could facilitate the capture of quantitative change of MeIAA during nodulation. First, I confirmed that overexpression of *IAMT1a* in hairy roots increased MeIAA levels (Fig. 15A). Then I detected the critical MeIAA peak especially in infected roots of *daphne* at 2 DAI (Fig. 16). I measured amounts of IAA and MeIAA at 0 DAI (non-inoculation) and 2 DAI in WT and *daphne*. Although no significant change in the amount of IAA or MeIAA could be detected in WT before or after rhizobial infection, a significant MeIAA increase after rhizobial infection was detected in *daphne* (Fig. 17A). Furthermore, I performed constitutive expression of *MES17*, which encodes the enzyme that converts MeIAA to IAA (Fig. 17B) (Yang et al. 2008), to counteract the catalytic function of *IAMT1a* during nodulation. Constitutive expression of *Lj2g3v2171910*, a gene homologous to *A. thaliana MES17* (Fig. 18), resulted in a statistically significant decrease in MeIAA levels and

nodule number compared to WT (Fig. 15B and 17C). These data indicate the importance of auxin methylation in nodule development. Furthermore, to gain insight into the role of auxin methylation, I tested the effect of exogeneous MeIAA on *NIN* expression. *NIN* is a key transcription factor of cortical cell division for nodule development (Soyano et al. 2013). Treatment with IAA did not induce *NIN* expression in *L. japonicus* roots (Fig. 17D), consistent with findings of Soyano et al. (2019) (Soyano et al. 2019). However, treatment with MeIAA did induce *NIN* expression (Fig. 17D). This induction of expression was not detected in *daphne* (Fig. 17E), suggesting that MeIAA affects cortical *NIN* expression. Finally, *NIN* expression was induced at 7 DAI in hairy roots harboring control vectors, but was poorly induced in hairy roots harboring *IAMT1a*-RNAi constructs (Fig. 17F). These findings indicate that auxin methylation by *IAMT1a* is involved in nodule development by affecting *NIN* expression.

2.3 Discussion

IAMT1 has been characterized as a gene encoding carboxy methyltransferase, which specifically converts IAA to MeIAA *in vitro* (D'Auria et al. 2003; Takubo et al. 2020; Zubieta et al. 2003). In *A. thaliana*, a non-symbiotic plant, *IAMT1* participates in MeIAA biosynthesis *in vivo* (Abbas et al. 2018), and in shoot development and differential growth (Abbas et al. 2018; Qin et al. 2005). On the other hand, the function of *IAMT1* in roots is unknown. This study demonstrates that *L. japonicus IAMT1* functions in root nodule development. I found an *IAMT1* gene duplication in the Fabaceae lineage and characterized one of two *IAMT1* genes, named *IAMT1a*, induced in roots after rhizobial infection, as a positive regulator of nodule development. Notably, I identified the increase

of MeIAA in roots after rhizobial infection using *daphne* (Fig. 17A). Because MeIAA is much less abundant than IAA (Abbas et al. 2018), a quantitative change of endogenous MeIAA in biological processes has not been reported. In this study, however, the use of *daphne* allowed me to detect for the first time, a significant increase of MeIAA levels associated with induction of *IAMT1a* expression mediated by rhizobial infection.

I documented induction of *IAMT1a* expression in nodulation using time-course RNA-seq in early symbiotic stages using *daphne*. *IAMT1a* is one of the most significant genes in a cluster of DEGs that are transiently induced in WT roots, but continuously and more strongly expressed in *daphne* roots after rhizobial infection (Fig. 3B). Consistent with changes of *IAMT1a* transcript levels detected using RNA-seq and qRT-PCR, upon epidermal infection, *IAMT1a* promoter activity is transiently observed in a local infectable region, but not throughout entire roots in WT, whereas it is persistently observed in wide regions of *daphne* roots (Fig. 4D, 6, and 8). *daphne* lacks the promoter region of *NIN* expression in cortex (Yoro et al. 2014), and the *nin* null mutant shows persistent expression of *IAMT1a*, as well as in *daphne* (Fig. 6), suggesting that characteristic spatiotemporal expression patterns of *IAMT1a* in *daphne* result from a lack of cortical *NIN*. Cortical *NIN* provides negative feedback and suppresses persistent, widespread epidermal infection (Liu et al. 2019; Suzaki et al. 2014; Yoro, Suzaki, and Kawaguchi 2019). *Early nodulin 11* is extensively expressed in *Mtnin-1* mutant (Marsh et al. 2007). Given this evidence, *IAMT1a* expression is probably under negative feedback control by cortical *NIN*.

A BLAST search of legumes and phylogenetically closely related non-legumes showed that legumes have two *IAMT1* genes, and a phylogenetic tree suggested that *IAMT1a* and *IAMT1b* genes originated from *IAMT1* duplication in the common

ancestor of legumes (Fig. 4C). IAMT1b, which shares 90% amino acid sequence identity with IAMT1a, also has a conserved amino acid sequence for the auxin-binding pocket (Fig. 5). Although it is assumed that both have the same molecular function, mRNA levels of *IAMT1a* are approximately 400-fold higher than those of *IAMT1b* in inoculated roots (Fig. 4D). *IAMT1a*, but not *IAMT1b*, is induced after rhizobial infection (Fig. 4D, 6, and 7). The reason for *IAMT1a*'s involvement in nodule symbiosis and not *IAMT1b's* may lie in the IAMT1a locus. Recently, the existence of genomic clusters, termed symbiotic islands, where symbiotic genes are concentrated, has been found in *Medicago* (Pecrix et al. 2018). The clustering of symbiotic genes is likely to contribute to coordinated gene regulation in nodule symbiosis, as genes with coordinated expression tend to be linked by location on the genome in eukaryotes (Hurst, Pál, and Lercher 2004). In the *L. japonicus* MG-20 ecotype, *IAMT1a* is located on chromosome 2 while *IAMT1b* is on chromosome 6. In the case of Gifu ecotype, *IAMT1a* is located on chromosome 1. There is a translocation between chromosome 2 of MG-20 and chromosome 1 of Gifu (Hayashi et al. 2001), where some symbiotic genes, *such as NIN*, *NUP133*, and *NFR1* are concentrated (Sandal et al. 2006). Therefore, the IAMT1a locus may be attractive for involvement in nodule symbiosis. The establishment of a new gene locus through a gene duplication in *IAMT1* may contribute to auxin methylation in nodule symbiosis. Considering that Arabidopsis *IAMT1* is required for development and differential growth in shoots, and that its functions in leaf development and gravitropic reorientation in hypocotyls (Abbas et al. 2018; Qin et al. 2005), *IAMT1b* may have inherited the function of *IAMT1* in shoots of non-legumes.

Auxin is involved in various processes in nodule symbiosis. During early infection stages, auxin biosynthesis occurs in epidermis, and auxin signaling has been

observed in infected epidermis (Nadzieja et al. 2018). A*uxin response factor (ARF) 16a* participates in IT formation (Breakspear et al. 2014). During the post-cortical cell division stage, *LjYUCCA1*/*MtYUC8* and *LjYUCCA11*/*MtYUC2*, encoding auxin biosynthetic enzymes, are expressed (Schiessl et al. 2019; Shrestha et al. 2020), and these are downstream factors of *SHORT INTERNODES /STYLISH (STY)*, required for nodule emergence (Shrestha et al. 2020). *GmYUC2a* is induced after rhizobial infection and is involved in nodule formation (Wang et al. 2019). Post-transcriptional control via miR160 regulates *ARF10/16/17* in soybean (Nizampatnam et al. 2015) and *Medicago* (Bustos-Sanmamed et al. 2013) in nodule developmental stages.

Considering that auxin biosynthesis occurs in epidermis during early stages of infection, auxin accumulation in epidermis may provide a substrate for IAMT1a *in vivo*. As evidence to support this, MeIAA levels showed an increasing trend in WT and were significantly elevated in *daphne* due to rhizobial infection (Fig. 17A), where *IAMT1a* is extensively expressed (Fig. 8F). In the beginning, I assumed the involvement of *IAMT1a* in epidermal events, such as IT formation. However, unexpectedly, *IAMT1a* knockdown had no effect on IT number, but inhibited nodule and primordium development involving cortical infection (Fig. 10 and 11). These findings indicate that *IAMT1a* is involved in cortical events for nodule development. Consistent with this result, spontaneous nodulation with constitutive expression of $CCaMK^{T265D}$ (a gain-of-function type of *CCaMK* (Tirichine et al. 2006; Yano et al. 2008)) was inhibited by *IAMT1a*-KD (Fig. 12). Since the *ccamk* mutant shows no induction of *IAMT1a* expression after infection (Fig. 6), *IAMT1a* is positioned as a downstream factor of *CCaMK*. On the other hand, spontaneous nodulation in the *snf2* mutant (a gain-of-function mutant of *LHK1* (Tirichine et al. 2007)) was not significantly inhibited by *IAMT1a*-KD (Fig. 12). Given that *LHK1*

expression in cortex, but not epidermis is sufficient to restore bump formation in *lhk1* mutants in the absence of rhizobial infection (Miri et al. 2019), although *LHK1* is expressed in epidermis and cortex (Held et al. 2014), *IAMT1a* can act either in parallel with or upstream of cytokinin signaling via *LHK1* in cortex.

A. thaliana MES17 has been identified as a MeIAA esterase *in vitro* (Yang et al. 2008). Constitutive expression of the homolog in *L. japonicus* decreased endogenous MeIAA levels and nodule number (Fig. 15B and 17C). Nodule development was inhibited by *IAMT1a* knockdown (Fig. 10) and further enhanced by its overexpression in *tml* background (Fig. 13 and 14). These results show that auxin methylation is an important process during nodule development. It is interesting to note that MeIAA has different properties from those of IAA. Soyano et al. (2019) found that expression of *NIN* is not induced by exogeneous IAA in *L. japonicus* (Soyano et al. 2019), and the present work confirmed that finding (Fig. 17D). In contrast, exogeneous MeIAA does induce *NIN* expression (Fig. 17D). Expression induction does not occur in *daphne* (Fig. 17E), which lacks the promoter region for cortical *NIN* expression, and *IAMT1a* knockdown inhibited *NIN* expression during the nodule developmental stage (Fig. 17F), suggesting that MeIAA contributes to induction of cortical *NIN* expression for nodule development.

Results of these experiments suggest that auxin methylation is not simply due to alteration of auxin homeostasis, and suggest following hypotheses. First, in intracellular signaling, MeIAA is a probable signaling molecule distinct from IAA. Since the IAA receptor, TIR1, recognizes the carboxyl group of IAA (Tan et al. 2007), MeIAA is not likely to be recognized by TIR1, which supports my hypothesis. Second, in intercellular signaling, MeIAA could have different mobility characteristics, as previous studies have noted (Li et al. 2008; Qin et al. 2005). MeIAA is a nonpolar molecule, unlike auxin and

other auxin conjugates. In general, non-polar molecules can penetrate cell membranes, but molecules such as ABA and glycerol, move via transporters. MeIAA rescues a part of phenotype of *Arabidopsis aux1* mutant (Li et al. 2008), suggesting that MeIAA can traverse the membrane or that it moves via the AUX1-independent influx system into cells, where it may work as a donor of IAA. During nodule development, it may be that MeIAA moves from epidermis into cortex and induces cortical *NIN*. MeIAA could migrate from epidermis to cortex, and be hydrolyzed in the cortex to produce IAA. Investigating this possibility and whether IAA can induce *NIN* in cortex are interesting issues for future research. Cortical cell division just below the epidermal cells infected with rhizobia is essential for symbiotic nodule formation. An analysis of auxin methylation and MeIAA function should open a new avenue for understanding the linkage between infection and development in nodule symbiosis.

2.4 Materials and Methods

Plant material and growth conditions

L. japonicus Miyakojima MG-20 ecotype (Kawaguchi 2000) was used as WT and the common genetic background for the following mutants: *ccamk-14* (Suzaki et al. 2019), *daphne*, *ern1*-6, *nin-9*, *snf2*, and *tml-4* (Miyazawa et al. 2010; Suzaki et al. 2012; Takahara et al. 2013; Yano et al. 2017; Yoro et al. 2014). 3-day-old seedlings were transferred to culture vessels containing sterilized vermiculite with B&D medium (Broughton and Dilworth 1971) and grown for 3 days for adaptation. Plants were then inoculated with *Mesorhizobium loti* MAFF303099 (DsRed-labeled for microscopic observation; (Maekawa et al. 2009)) suspended in B&D medium.

Time-course RNA sequencing

Roots of WT and *daphne* cultured without (0 DAI) or with inoculation (1, 2, and 3 DAI) were harvested. Total RNA was isolated using RNeasy Plant Mini Kit (QIAGEN) and with DNA removed by treatment with DNase (QIAGEN). Three independent biological replicates (each with n = 20 roots) were included for each time point. RNA-seq libraries were prepared using NEBNext Ultra II RNA Library Prep Kit for Illumina (NEB) and NEBNext Poly(A) mRNA Magnetic Isolation Module (NEB). Libraries were sequenced using an Illumina Hiseq 2000 and generated 66-bp single-end reads.

All RNA-seq reads were qualified by FastQC (ver. 0.11.3) and adapter trimmed with Trimomatic (ver. 0.33, options: CROP:66 LEADING:30 TRAILING:30 SLIDINGWINDOW:4:15 MINLEN:36). Trimmed reads were mapped to the MG-20 genome (Lj3.0 gene models) using Tophat2 (v2.1.0). The number of reads was calculated using HTseq (ver. 0.6.0), and was normalized using the trimmed Mean of M-values method in edgeR. Time-course DEGs were extracted using maSigPro.

The raw reads have been deposited in the DDBJ Sequence Read Archive (DRA) under accession number DRA013121.

Alignment and Phylogenetic tree construction

Alignment of sequences retrieved from the NCBI genome database and Phytozome v12 (https://phytozome.jgi.doe.gov/pz/portal.html), was performed using Clustal X. Poorly aligned regions were automatically removed by trimAl (Capella-Gutiérrez, Silla-Martínez, and Gabaldón 2009). Phylogenetic trees were estimated by the maximum likelihood method and constructed using the trimmed amino-acid sequence and IQ-TREE

(Nguyen et al. 2015). ModelFinder (Kalyaanamoorthy et al. 2017) was used for model selection.

Expression analysis

Primers used for qPCR are listed in Table 1. Roots were harvested for RNA extraction using PureLink Plant RNA reagents (Invitrogen). After treatment with DNase I (Takara) to remove genomic DNA, cDNA was synthesized from < 0.1 μg of RNA using ReverTra Ace qPCR RT Master Mix (Toyobo). Quantitative PCR was performed with Thunderbird SYBR qPCR Mix (Toyobo) on a Roche LightCycler 96 system (Roche) according to the manufacturer's protocol. Expression of *LjUBQ* was used as a reference.

Plasmid construction and Transformation

To effect knockdown (KD), overexpression (OX), and promoter-GUS reporter assay of *LjIAMT1a* (*Lj2g3v3222870*), partial-length or full-length cDNA and 2.9 kbp upstream sequence were amplified by PCR with primers containing an extra 5′-CACC sequence and cloned into the pENTR/D-TOPO vector (Invitrogen). The coding sequence of *LjMES17* (*Lj2g3v2171910*) was cloned as well. The primers are listed in Table 1. Entry vectors were recombined into modified Gateway binary vectors pro*LjUBQ*:GWS-GFP, pro*LjUBQ*:GW-GFP, or pMDC162-GFP.

Transgenic hairy roots were induced using *Agrobacterium rhizogenes* AR1193. MG-20 4-day-old seedlings (grown for 3 days in the dark and for 1 day in 16 h light/8 h dark, 24°C) were cut off below the hypocotyls while immersed in *A. rhizogenes* suspension carrying the corresponding vectors. These were co-cultivated in 1/2 strength B5 medium (Wako) including 0.02 g L^{-1} sucrose, 0.5 g L^{-1} MES, and 0.9% agar at 24 °C

in the dark for 3 days, and were transferred to hairy root induction medium (B5 medium with 1% sucrose, Gamborg B5 vitamins solution, 0.5 g L^{-1} MES, 12.5 μg mL^{-1} meropenem (Sumitomo Pharmaceuticals), and 0.9% agar) for 10-14 days in 16 h light/8 h dark, 24°C. Plants with transgenic hairy roots were inoculated with rhizobia 3-5 days after transfer to vermiculite.

Microscopy

Bright-field and fluorescence microscopy were performed with a BX50 upright microscope (Olympus) or with an A1R confocal microscope (Nikon). Images were acquired and analyzed using DP Controller (Olympus), NIS Elements (Nikon).

Histochemical analysis

Hairy roots of WT and *daphne* were transformed with the β-glucoronidase (GUS)-reporter gene fused to the *IAMT1a* promoter. Roots were incubated in the histochemical GUS staining solution (100 mM $NaPO_4$ (pH 7.0), 0.5 mg mL^{-1} 5-bromo-4-chloro-3-indolyl-β-glucuronic acid, 2 mM $K_4Fe(CN)_6$, 2 mM $K_3Fe(CN)_6$, and 0.1% Triton X-100) for < 60 min at 37 °C after 10 min vacuum filtration.

Quantification of IAA and MeIAA

Forty roots were harvested in each biological replicate of WT and *daphne*. For preparation of plant extracts, frozen plant material was dissolved in 400 μL of 80% MeOH containing 60 pmol [$^2H_5$]-MeIAA in a tube, pulverized using a Multibead shocker (Yasui kikai) for 2 min at 1500 rpm and 4 °C. After centrifugation for 3 min at 13,000 rpm and 4 °C, 300 μL of the supernatant were transferred to another tube. Then 300 μL of hexane were added.

After vortexing and centrifugation at 15,000 rpm for 5 min, the lower layer was collected, dried using a centrifugal evaporator, and dissolved in 20 μL of 80% MeOH after centrifugal evaporation. Mass spectroscopy analysis was performed using a Triple TOF 5600 mass spectrometer (AB SCIEX), coupled with a micro 200 LC system (SCIEX). Metabolites were separated using a HALO fused C_{18} column (500 μm id × 5 cm, 2.7 μm particles) with gradient elution of mobile phase A (0.5% formic acid/H_2O) and mobile phase B (methanol) (0 min: 5% B; 10 min: 95% B; 13 min: 95% B) at an eluent flow rate of 25 μL/min and RT. The mass spectrometer was operated in ESI positive-mode ionization with Multiple Reaction Monitoring (MRM). MRM transitions are *m/z* 190.1 to 130.106 for MeIAA, *m/z* 176.2 to 130.06 for IAA and *m/z* 195.1 to 135.11 for [$^2H_5$]-MeIAA. Source parameters are curtain gas, 25psi; spray voltage, 5.5 kV; temperature, 550°C; ion source gas 1, 25psi; ion source gas 2, 35psi.

Application of MeIAA and IAA

With reference to Yang et al. (2008) (Yang et al. 2008), MeIAA and IAA dissolved in 95% ethanol were diluted 1:1,000 in medium to a final concentration of 10^{-7} M. 5-day-old seedlings transferred to beakers containing either MeIAA or IAA were incubated at RT in dark, based on Murray et al. (2007) (Murray et al. 2007). After 24 h, roots were harvested to analyze gene expression.

2.5 Figures

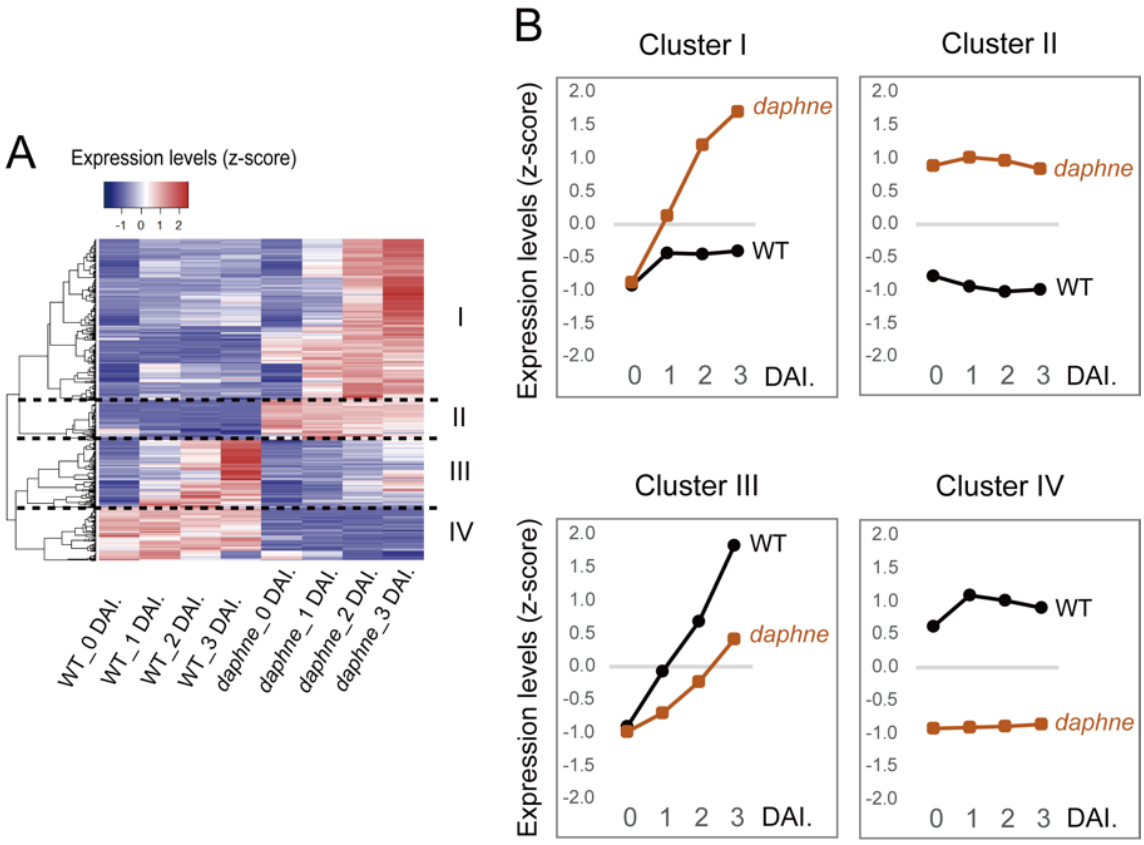

Figure 3. Time-course RNA-seq in WT and *daphne*. (A) Classification of DEGs with fold change > 2 (1181 genes) into four subgroups (I to IV) by hierarchical clustering. **(B)** Expression modules of genes with significant differences between WT (black line) and *daphne* (orange line) during early infection. Each dot in each cluster represents an average value.

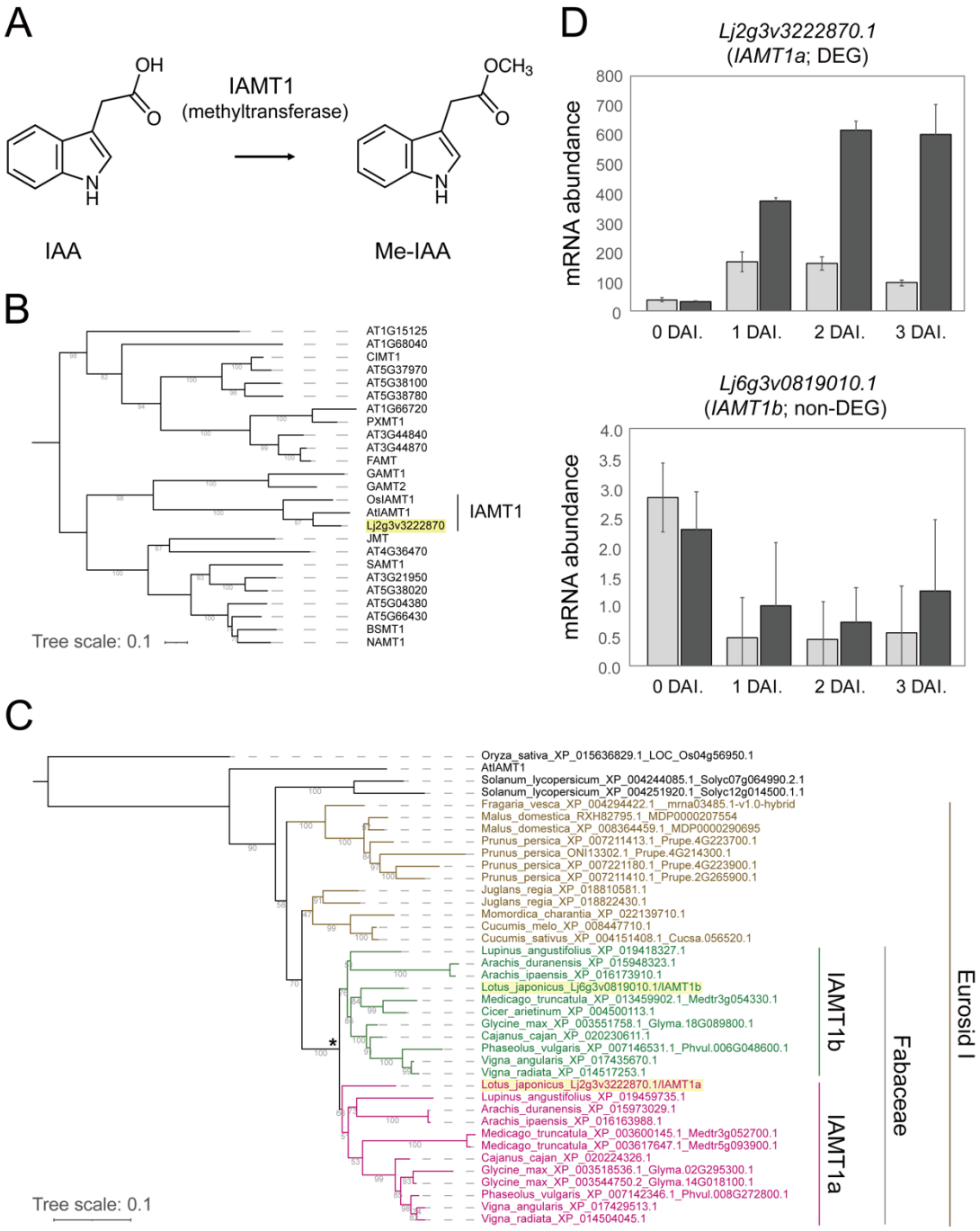

Figure 4. **Expression patterns of two *IAMT1* genes in *L. japonicus* and phylogenetic trees containing these genes. (A)** *A. thaliana* IAMT1 specifically converts IAA into MeIAA *in vitro* (D'Auria et al. 2003; Takubo et al. 2020; Zubieta et al. 2003). **(B)** Phylogenetic tree of *A. thaliana* carboxyl methyltransferases in the SABATH family,

including OsIAMT1 (Zhao et al. 2008), and Lj2g3v3222870. **(C)** Fabaceae lineage-specific duplication of *IAMT1*. An asterisk indicates the duplication in the Fabaceae. **(D)** *Lj2g3v3222870* (*LjIAMT1a*), but not *Lj6g3v0819010* (*LjIAMT1b*) was detected as a differentially expressed gene (DEG) in time-course RNA-seq analysis. mRNA abundance of WT (gray bars) and *daphne* (black bars) in *LjIAMT1a* and *LjIAMT1b* at 0 (non-inoculation), 1, 2, and 3 DAI. Error bars indicate means ± SDs of three biological replicates.

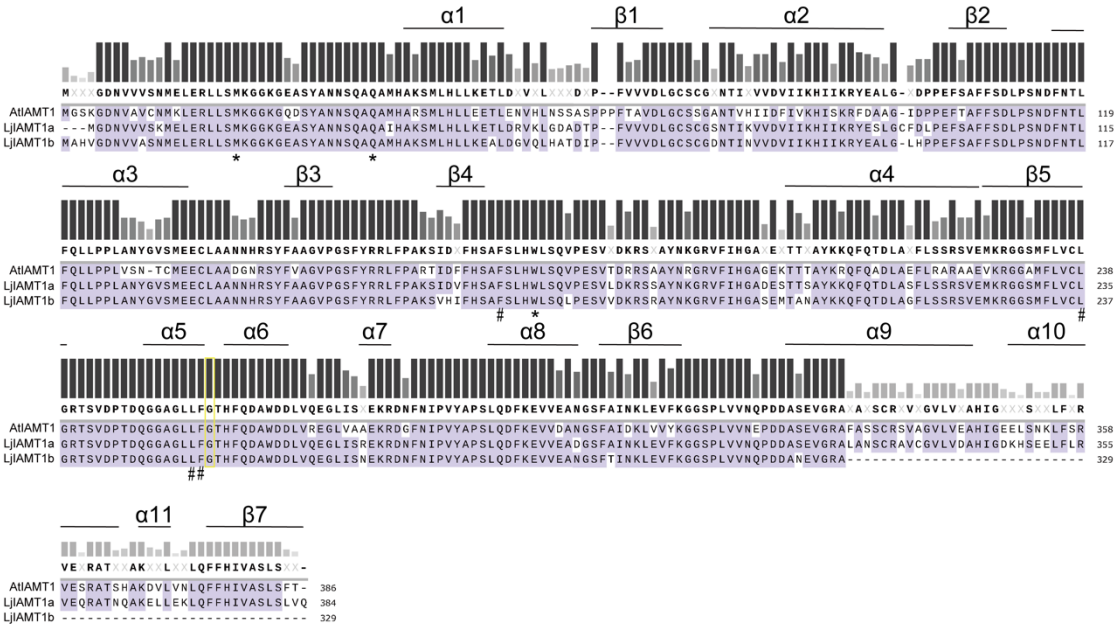

Figure 5. Amino-acid sequences of full length IAMT1 proteins in *A. thaliana* and *L. japonicus*. Residues with "#" interact with the aromatic moiety of the substrate and are important for substrate selectivity, and residues with asterisks interact with the carboxyl moiety of IAA (Zhao et al. 2008; Zubieta et al. 2003). Gly-256, surrounded by a yellow rectangle, of *A. thaliana* IAMT1 is characterized as a pocket for recognition and binding of the indole ring of IAA (Zhao et al. 2008; Zubieta et al. 2003).

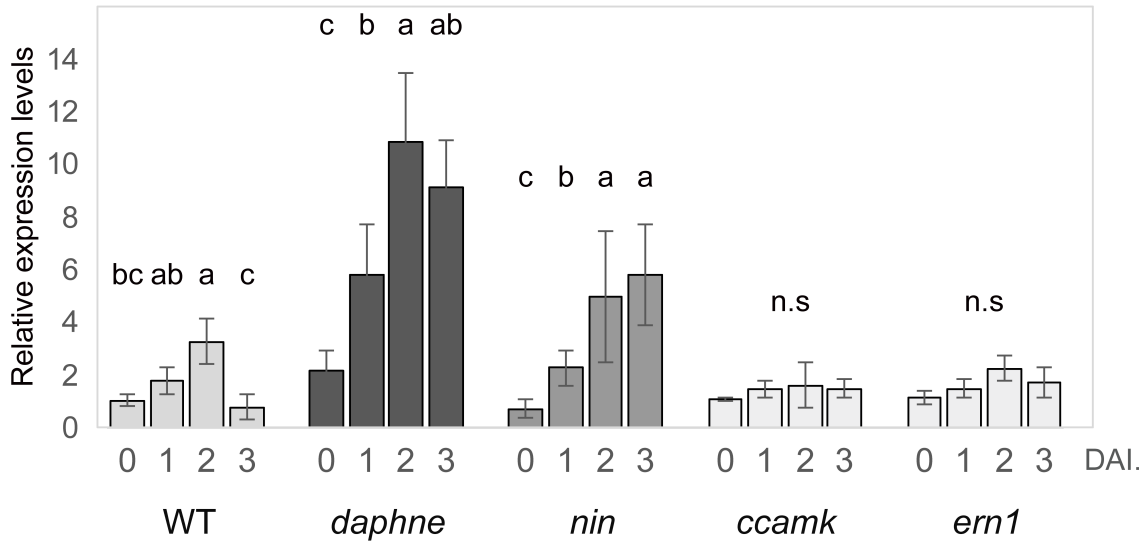

Figure 6. Genetic dependencies of *IAMT1a* expression in the early infection stage. Time-course qRT-PCR analysis of *IAMT1a* expression in WT, *daphne*, *nin-9*, *ccamk-14*, and *ern1-6* at 0 (non-inoculation), 1, 2, and 3 DAI. Data are means of three or more biological replicates and displayed as values relative to WT at 0 DAI. Error bars indicate means ± SDs (n = 12 plants for each biological replicate). Statistical analysis was performed using ANOVA followed by Tukey's honest significant difference (HSD) test ($p < 0.05$) in each genetic background. Different letters indicate significant differences. There were no significant differences (n.s.) in *ccamk-14* and *ern1-6*.

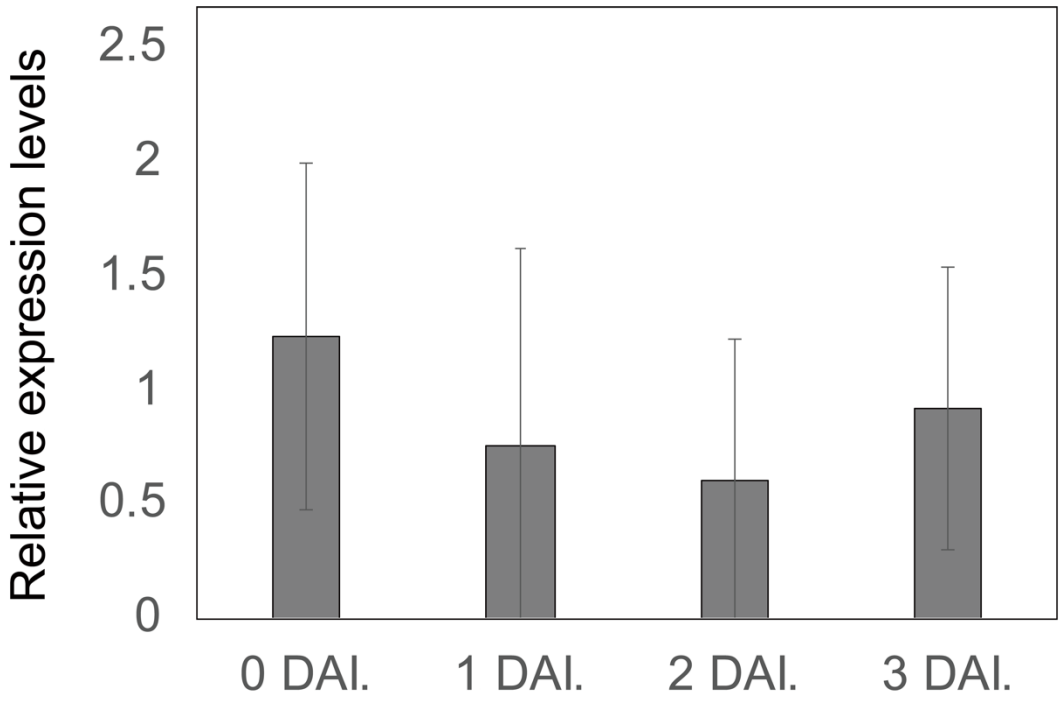

Figure 7. qRT-PCR analyses of *IAMT1b* expression in WT at 0 (non-inoculation), 1, 2, and 3 DAI. Data are means of five biological replicates and displayed values are relative to WT at 0 DAI. Error bars indicate means ± SDs (n = 12 plants for each biological replicate). ANOVA followed by Tukey's HSD test showed no significant differences among groups of time series.

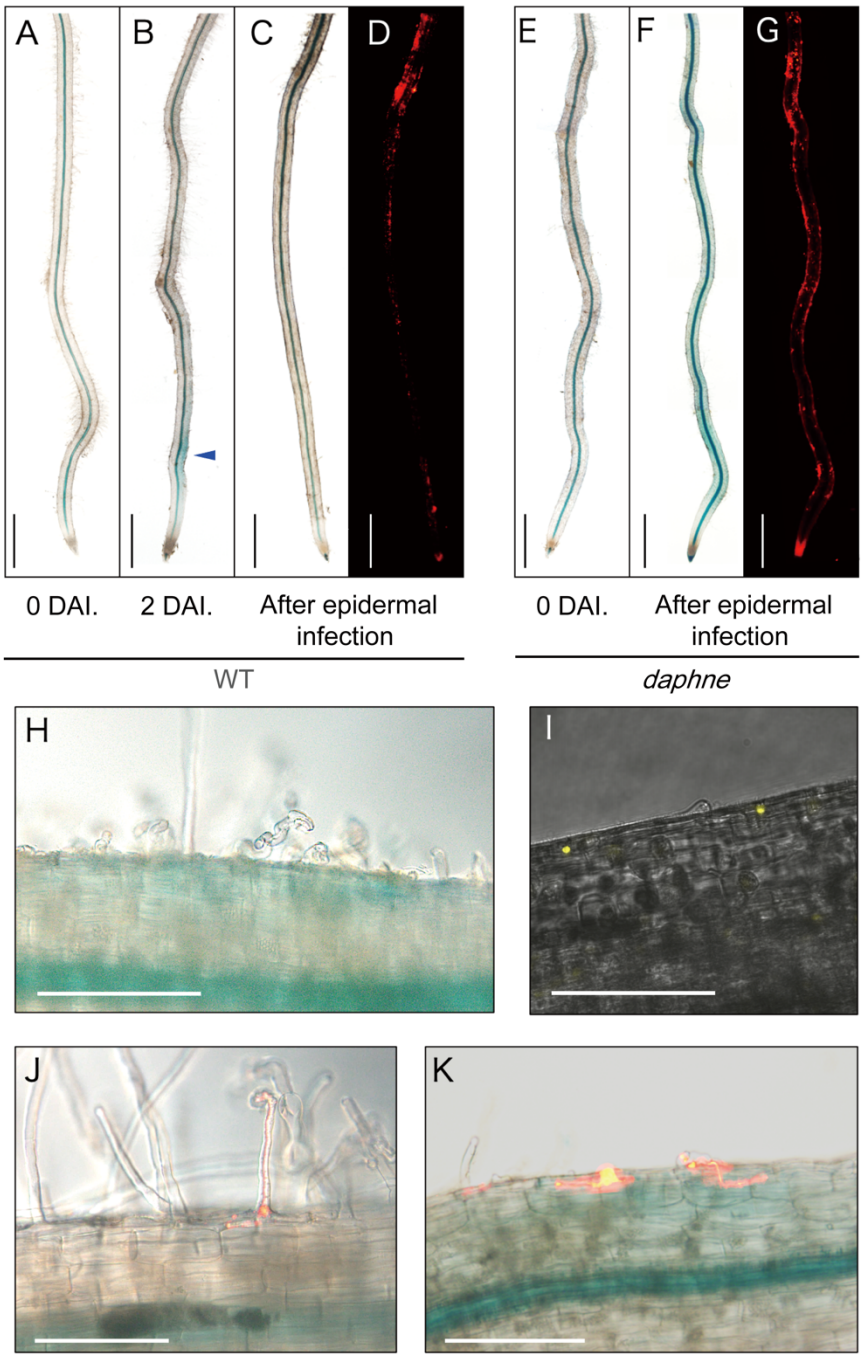

Figure 8. Spatiotemporal profile of *IAMT1a* expression in WT and *daphne* roots inoculated with or without rhizobia. WT (A to D, and H to J) and *daphne* (E to G, and K) roots were transformed with *proIAMT1a:GUS* or *proIAMT1a:tripleYFP-nls* (I). GUS activity was observed at 0 DAI. (non-inoculation; A and E), 2 DAI (B), and after ITs

developed (C and F). Arrowheads indicate active GUS sites in WT. DsRed-labelled *M. loti* was infected in epidermis (D and G). Magnified images of the susceptible region of WT at 2 DAI (H and I) and the root region where epidermal ITs were observed in WT (J) and *daphne* (K). Images merged with DsRed fluorescence are shown. Scale bar = 0.5 mm in (A to G); 100 μm in (H to K).

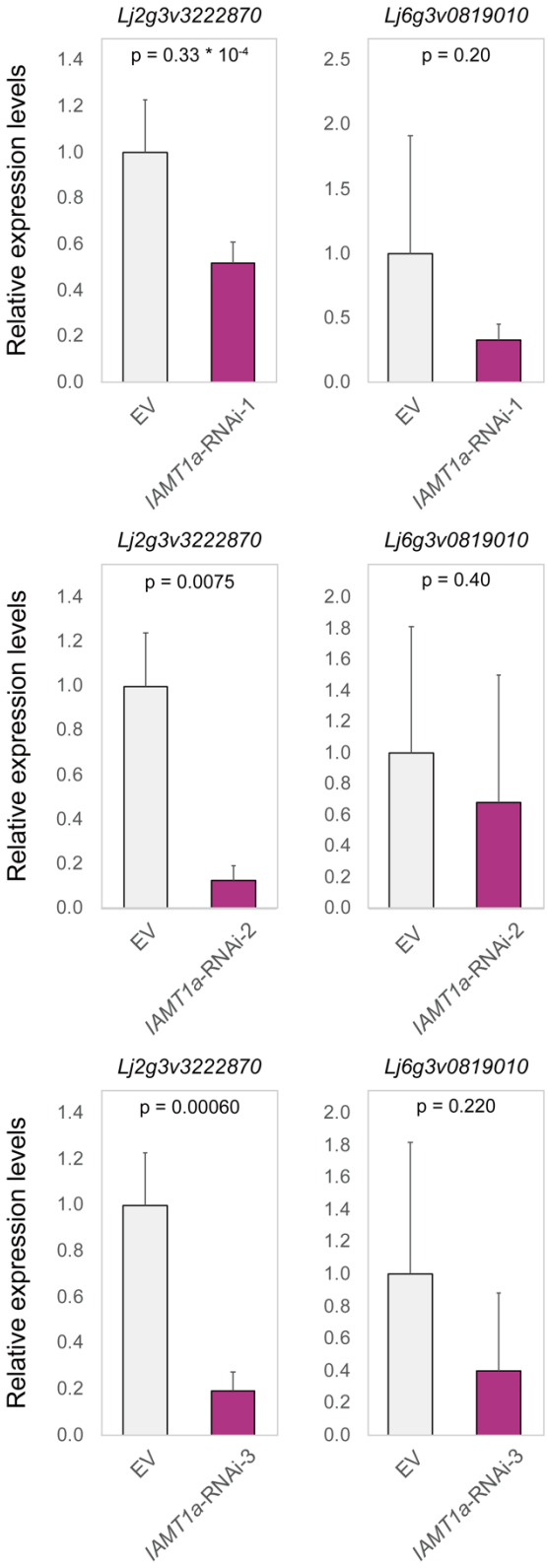

Figure 9. Effects of *IAMT1a*-RNAi on *IAMT1a* and *IAMT1b* transcripts. Relative expression levels of *IAMT1a* and *IAMT1b* in hairy roots of WT harboring EV controls (gray) or *IAMT1a*-RNAi vectors (pink) at 2 DAI. Values are means ± SDs for three biological replicates). n > 10 hairy roots for each biological replicate.

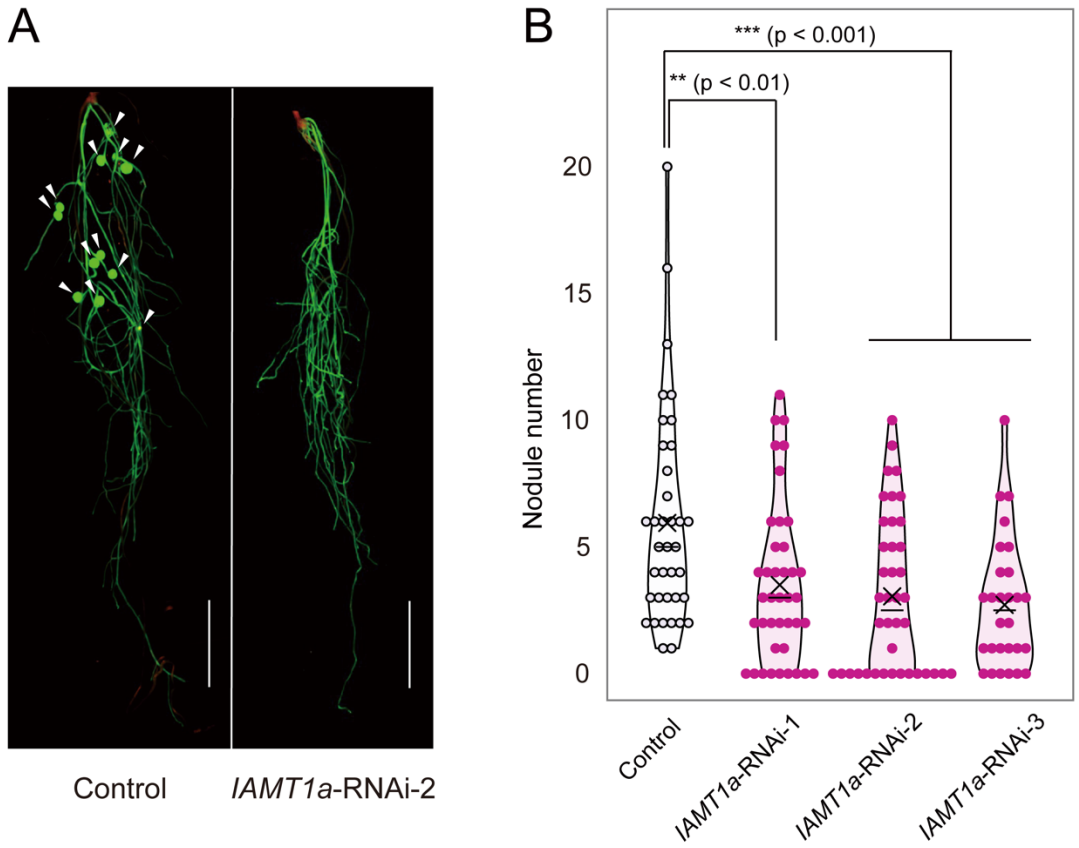

Figure 10. *IAMT1a*-RNAi inhibits nodulation. (A) Representative phenotype of hairy roots of WT harboring an empty vector (EV) as a control (left) and the *IAMT1*-RNAi-2 vector (right) 3 weeks after inoculation. Roots expressing GFP as a transformation marker were selected. Root nodules are indicted by arrowheads. Scale bar = 1 cm. **(B)** The nodule number in hairy roots harboring EV (controls) and IAMT1-RNAi vectors 3 weeks after inoculation. Each dot represents the nodule number of each plant. n = 37 (control), 40 (RNAi-1), 40 (RNAi-2), and 28 (RNAi-3). Asterisks indicate that differences are statistically significant (Welch's t-test).

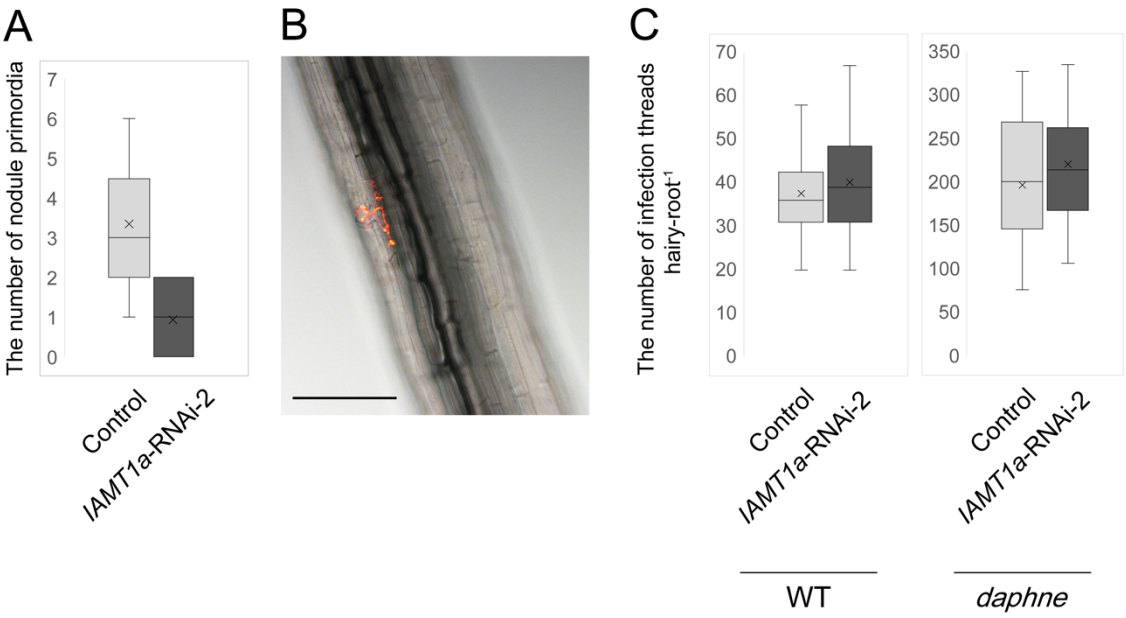

Figure 11. *IAMT1a*-RNAi affects formation of nodule primordia rather than epidermal infection. (A) The number of nodule primordia in hairy roots harboring EV as controls (light gray, n = 17) or *IAMT1a*-RNAi-2 vectors (dark gray, n = 16) in WT at 7 DAI. **(B)** Representative images of an infection thread aborted in epidermis of *IAMT1a*-RNAi hairy roots with no nodules, 3 weeks after inoculation. Roots expressing GFP as a transformation marker were selected. DsRed-labeled *M. loti MAFF303099* was used for microscopic observation. Scale bar = 100 μm. **(C)** The number of infection threads in hairy roots harboring EV as controls or *IAMT1a*-RNAi-2 vectors in WT (light gray) and *daphne* 10 days after inoculation (dark gray). n = 28 (control/WT), 29 (RNAi/WT), 28 (control/*daphne*), and 25 (RNAi/*daphne*).

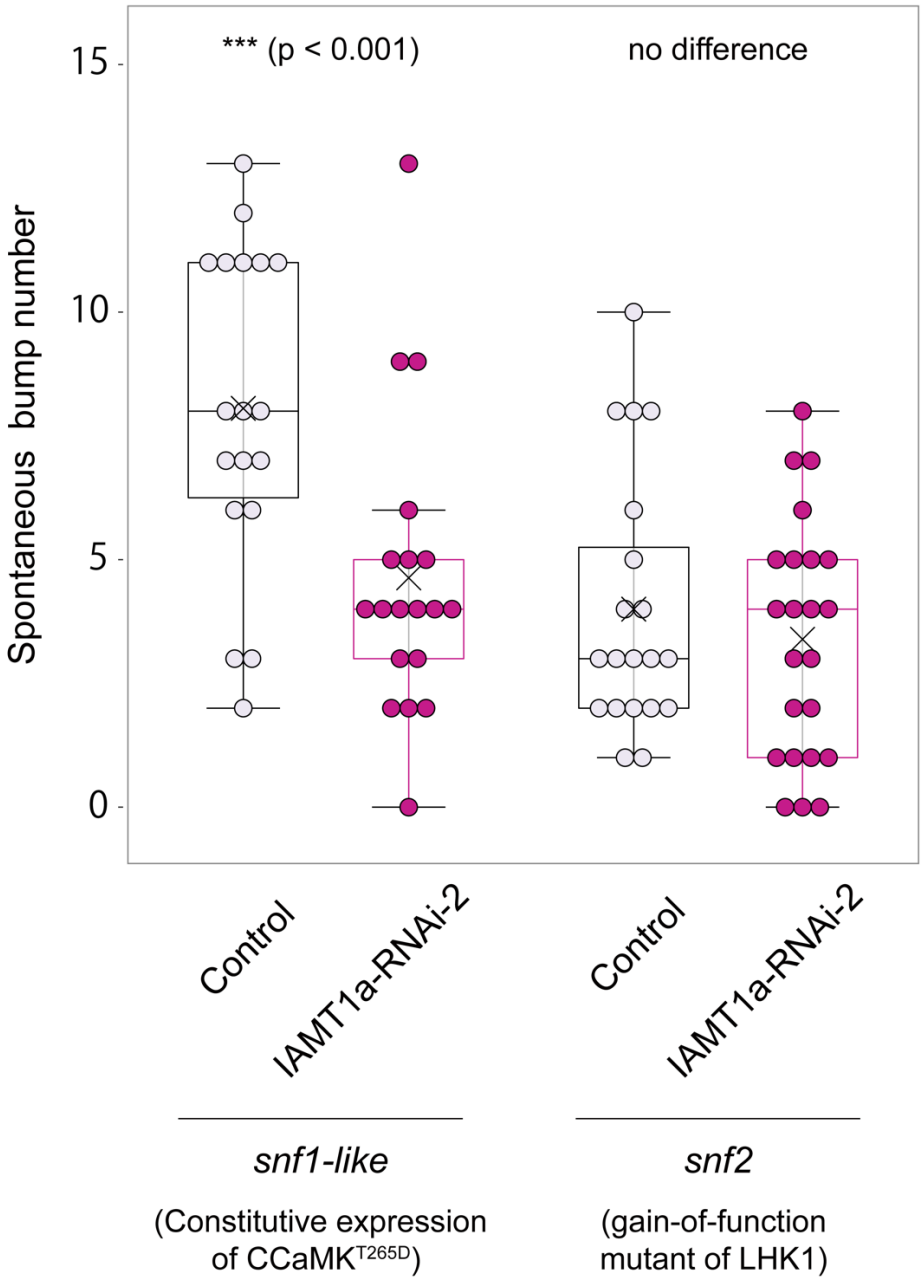

Figure 12. *IAMT1a*-RNAi inhibited spontaneous nodule formation. *snf1-like* (left) and *snf2* (right) have transgenic hairy roots containing *IAMT1*-RNAi vectors or EV controls. Successful transgenic plants were transferred to vermiculite and grown for about a month. Each dot represents the spontaneous bump number of each plant. n = 18 (control/*snf1-like*), 19 (RNAi/*snf1-like*), 20 (control/*snf2*), and 23 (RNAi/*snf2*). Asterisks

indicate statistically significant differences (Welch’s t-test).

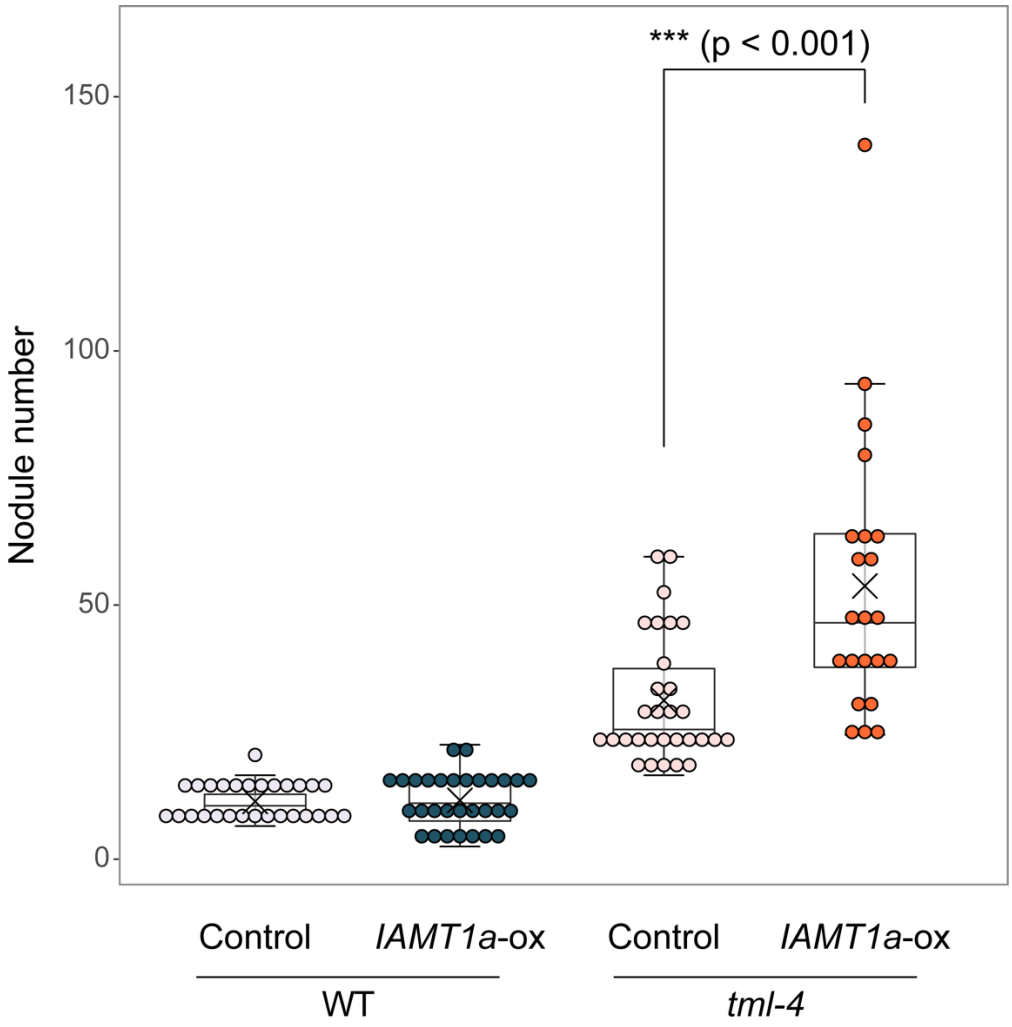

Figure 13. *IAMT1a* overexpression promotes nodulation. Transgenic hairy roots harboring the *proLjUBQ:IAMT1a* vector and EV control were generated in WT (left) and *tml-4* mutant (right). Nodules were counted 3 weeks after inoculation. Each dot represents the nodule number of each plant. n = 28 (control/WT), 30 (ox/WT), 30 (control/*tml-4*), and 22 (ox/*tml-4*). Asterisks indicate that differences are statistically significant (Welch's t-test).

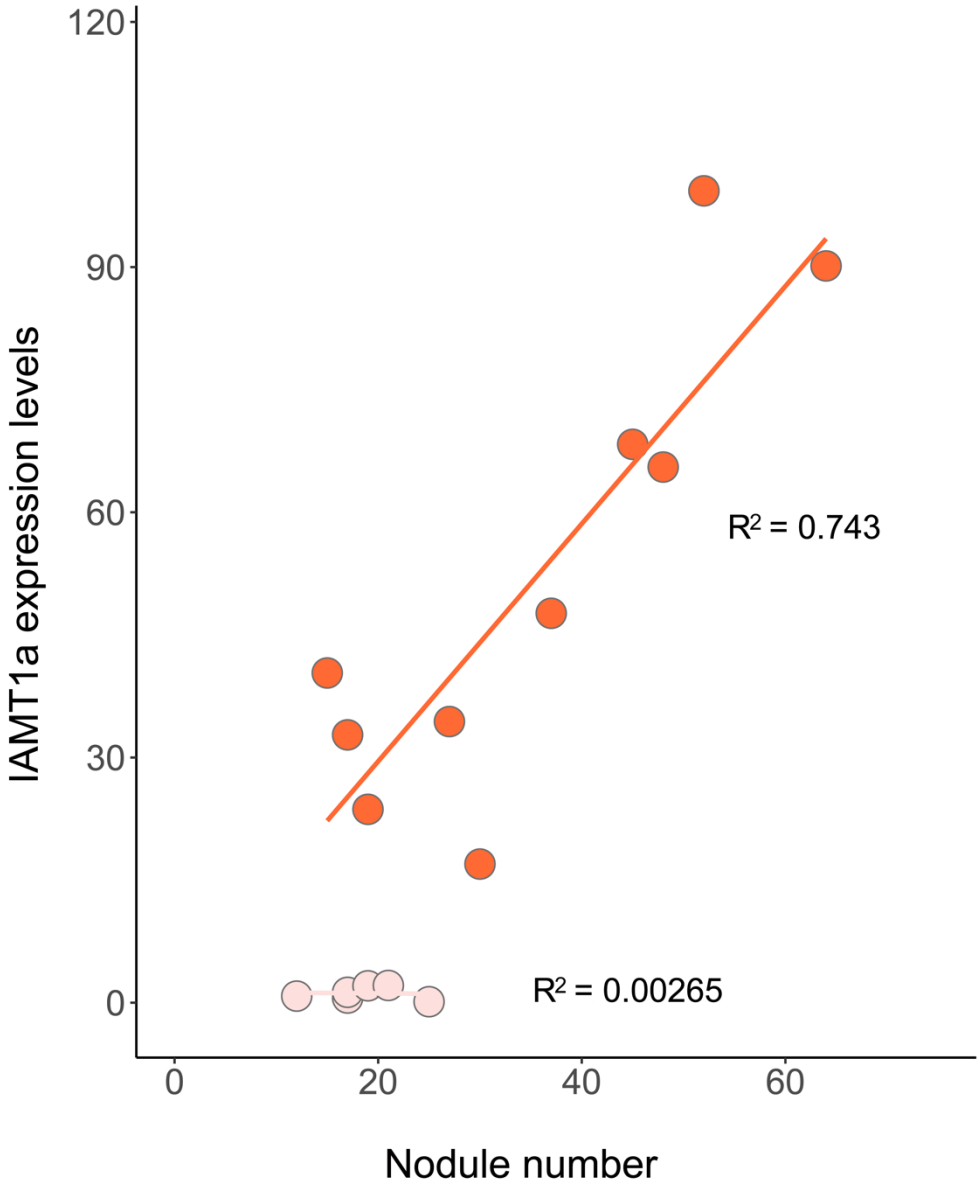

Figure 14. Correlation between the level of *IAMT1a* transcripts and the number of nodules. Hairy roots of *tml-4* harboring EV controls (lower, n = 6) and *proLjUBQ:IAMT1a* vectors (upper, n = 10). R^2 = 0.00265 and 0.743 in controls and *IAMT1a* overexpression roots, respectively.

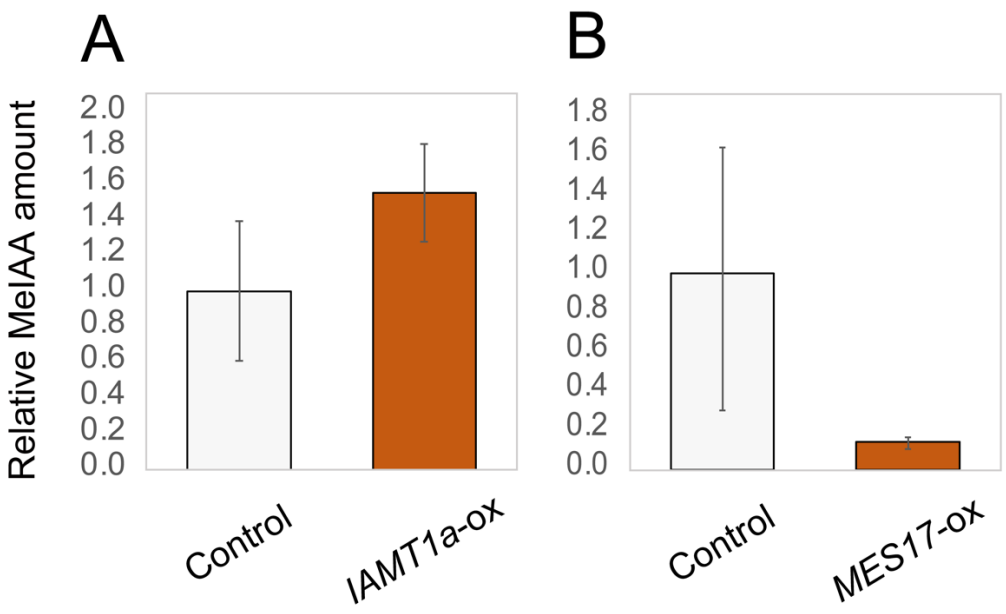

Figure 15. Changes of MeIAA amounts by *IAMT1a* and *MES17* overexpression. Transgenic hairy roots that contained *IAMT1a*-ox vector (A), *MES17*-ox vector (B) or EV control, were used. Error bars indicate means ± SDs of three biological replicates (n = 30 hairy roots for each biological replicate).

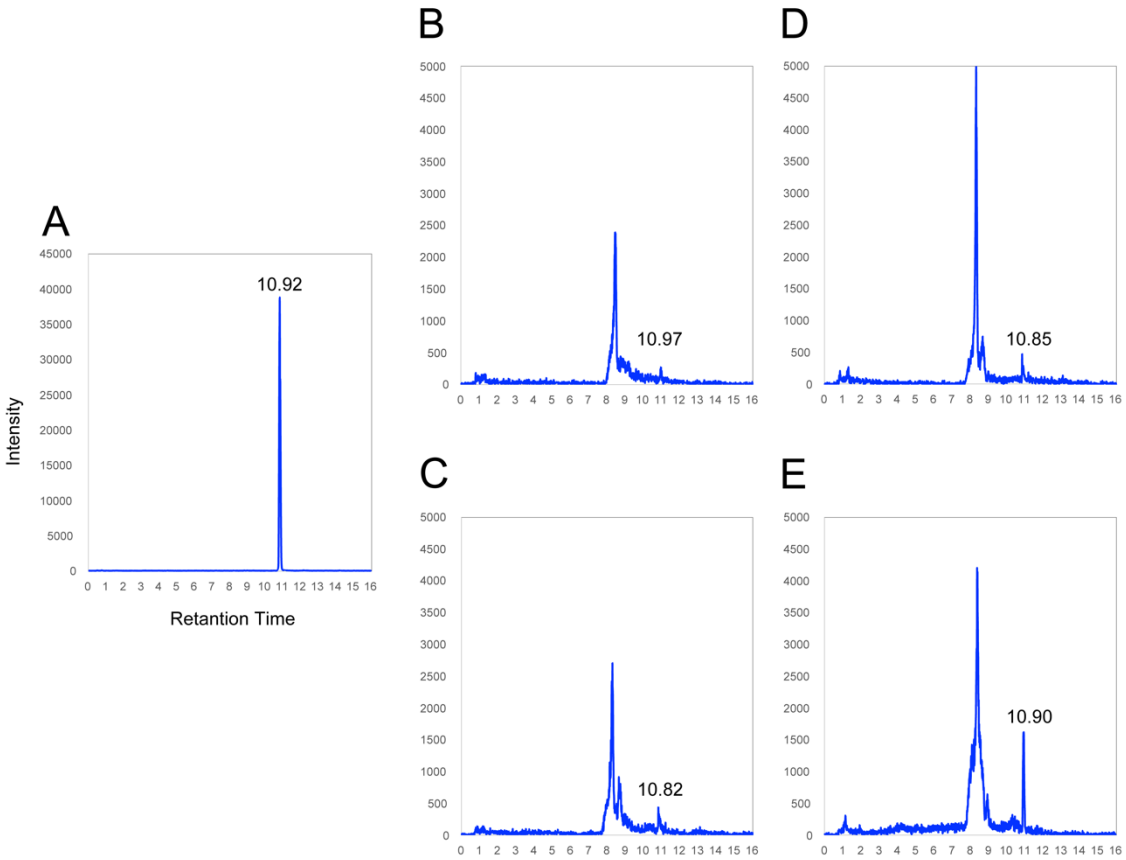

Figure 16. MeIAA detection with or without rhizobial infection. Mass spectra by mass spectrometry analysis in standard (A), in WT (B and C), and *daphne* (D and E) at non-inoculation (B and D) and 2 DAI (C and E). Peaks marked with a value correspond to MeIAA.

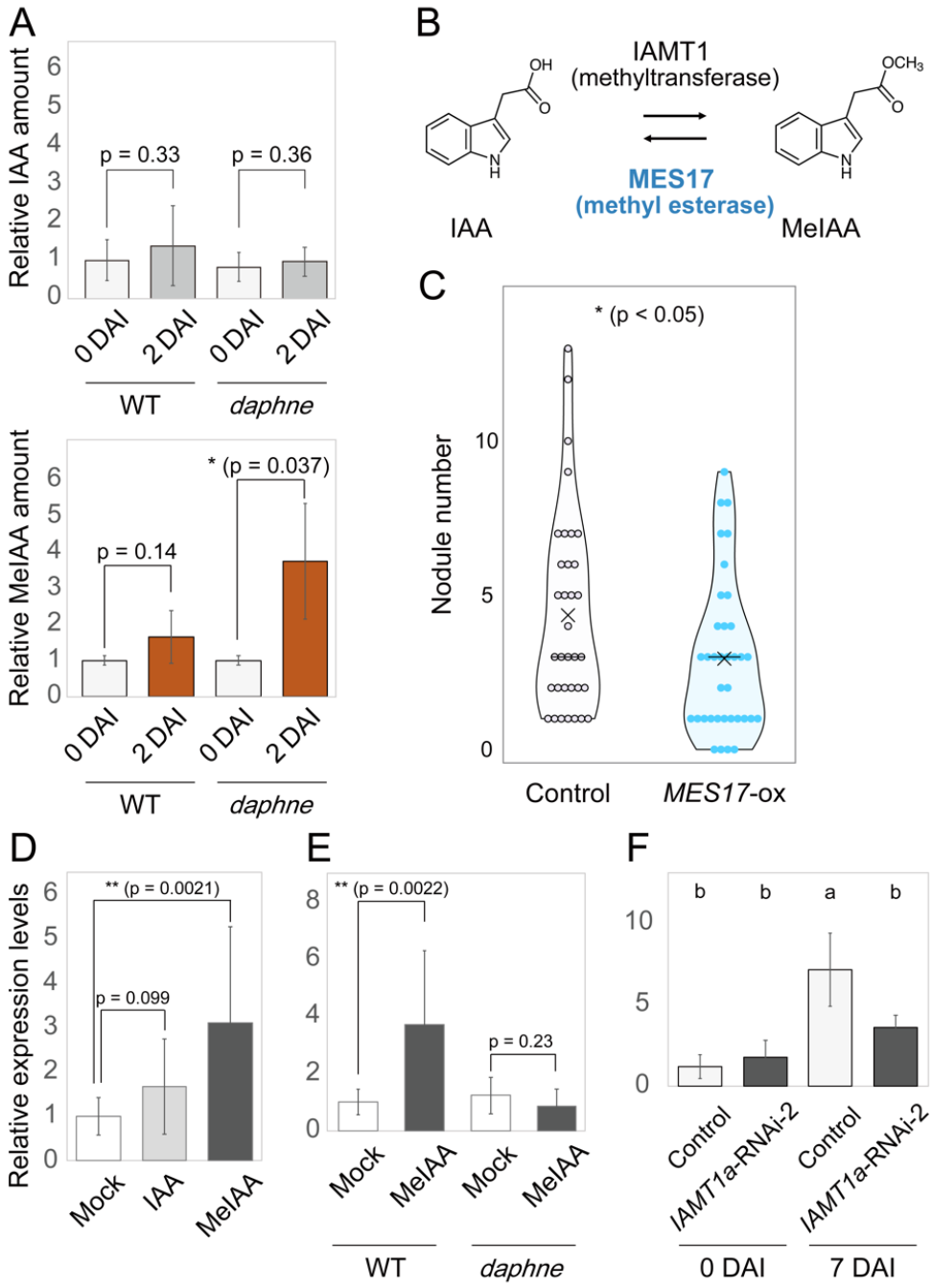

Figure 17. Auxin methylation and *NIN* expression. (A) Relative amount of IAA and MeIAA at 0 DAI (non-inoculation) and 2 DAI in WT and *daphne*. Error bars indicate means ± SDs of three biological replicates (n = 40 plants for each biological replicate).

(B) MES17 demethylates MeIAA *in vitro* (Yang et al. 2008). **(C)** Nodule numbers in controls and constitutive expression of *LjMES17* 3 weeks after inoculation. Each dot represents the nodule number of each plant. n = 34 (control) and 36 (ox). **(D)** Relative expression levels of *NIN* after treatment with DMSO as mock, IAA (10^{-7} M), or MeIAA (10^{-7} M) for 24 h in WT. **(E)** Relative expression levels of *NIN* after treatment with DMSO as mock or MeIAA (10^{-7} M) for 24 h in WT and *daphne*. Error bars indicate means ± SDs of six biological replicates (n = 10 plants for each biological replicate) (D and E). Asterisks indicate that differences are statistically significant (Welch's t-test) (A, C, D and E). **(F)** Relative expression levels of *NIN* in hairy roots harboring EV as controls and *IAMT1a*-RNAi-2 vectors at 0 DAI (non-inoculation or 7 DAI. Error bars indicate means ± SDs of three or five biological replicates in control or RNAi, respectively (n > 10 hairy roots for each biological replicate). Statistical analysis was performed using ANOVA, followed by Tukey's honest significant difference (HSD) test ($p < 0.05$) in each genetic background. Different letters indicate significant differences.

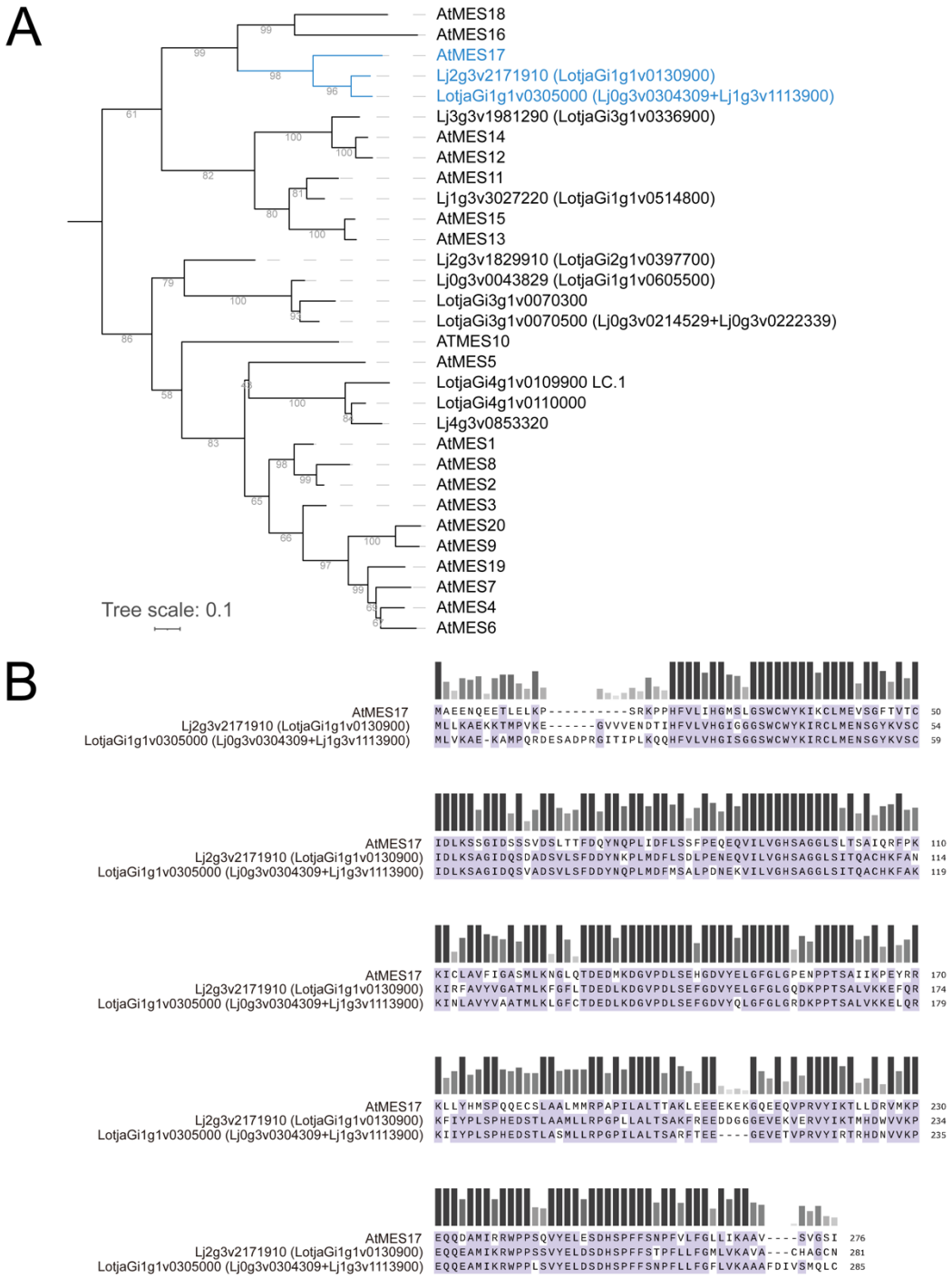

Figure 18. Phylogenetic tree and alignment of MES proteins. (A) Phylogenetic tree displaying *A. thaliana* and *L. japonicus* MES17s and other MES proteins. **(B)** Amino-acid sequences of full length MES17 proteins in *A. thaliana* and *L. japonicus*.

Table 1. Primers used in this study.

Name	Sequence (5' to 3')
UBQ qPCR (F)	ATGCAGATCTTCGTCAAGACCTTG
UBQ qPCR (F)	ACCTCCCCTCAGACGAAG
IAMT1a qPCR (F)	TCCCTCTTTTGTGTGTTGTTTGTGT
IAMT1a qPCR (R)	TCGTATTGTTTGTCACCACCAATCC
IAMT1b qPCR (F)	TTCATGCCACTGACATCC
IAMT1b qPCR (R)	GGGTGGAGTCCCAAAGC
NIN qPCR (F)	CAATGCTCTTGATCAGGCTGTTGA
NIN qPCR (R)	GAGTGCTAATGGCAAATTGTGTGTC
IAMT1a -RNAi-1 (F)	CACC CCAGCGACCAAATGAAAGTT
IAMT1a -RNAi-1 (R)	CTAGGATCACCCCAACTCCA
IAMT1a -RNAi-2 (F)	CACC CTACTTTGCTGCCGGAGTT
IAMT1a -RNAi-2 (R)	TCCCCAAGCAAACTAAGAACA
IAMT1a -RNAi-3 (F)	CACC TCCAAAATGGAACTTGAGAGG
IAMT1a -RNAi-3 (R)	ATTGCTGGGAAGGTCAGAGA
IAMT1a -OX (F)	CACC CATCCTTGTAGCATGCATGCG
IAMT1a -OX (R)	CTTCCACAAGATATGGACACTATCA
MES17 -OX (F)	CACC ATGCAAATGACCCTGA
MES17 -OX (R)	GCTTGTCCCCAAACAAATGT
proIAMT1a:GUS (F)	CACC ATTGCCCCAATGACACTACC
proIAMT1a:GUS (R)	TCGGAGCCAGAATTAAATAG

Chapter 3 GENERAL DISCUSSION

Evolution of nodule symbiosis, and a gene duplication of *IAMT1* in legume lineage

Nodule symbiosis is found in the nitrogen-fixing clade (Rosales, Cucurbitales, Fagales, and Fabales). However, it is ubiquitous in Fabaceae (legume) but limited in the others. In my study, a gene duplication of *IAMT1* in the legume lineages was suggested. Gene duplication can be a driving force in evolution (Ohno 1970). Therefore, a gene duplication of *IAMT1* in the legume lineage may have evolutionarily contributed to development of nodule symbiosis in the legume.

While most duplicated genes usually disappear, the estimated half-life of which is 3.2 million years for *A. thaliana* (Lynch and Conery 2000), some duplicated genes on an evolutionary trajectories toward stable situations. Regarding gene duplication scenarios, when duplicated genes become redundant, they can lead to pseudogenization, sub-functionalization, or neo-functionalization. In addition to divergence in protein function, divergence in expression pattern can be involved in the maintenance of duplicated genes (Doebley and Lukens 1998), and divergence in expression patterns has been suggested in experimental plant studies that leads to functional differentiation and novel functionalization (Kramer, Jaramillo, and Di Stilio 2004). In my study, *L. japonicus IAMT1a* shared a function with *A. thaliana IAMT1* in MeIAA biosynthesis. In contrast, expression patterns differed between the two: *A. thaliana IAMT1* is expressed and functions in shoot, while *L. japonicus IAMT1a*, generated by a gene duplication, was induced by rhizobial infection in roots and involved in nodule formation. *L. japonicus IAMT1b* was barely expressed in roots and not induced by rhizobial infection. Therefore,

a gene duplication of *IAMT1* would contribute to the divergence in expression pattern of *IAMT1*.

The evolutionary robustness of nodule symbiosis in legumes has been previously speculated to be associated with root-hair infection via IT, because it has been developed especially in the legume lineages. As for the entry modes of nitrogen-fixing bacteria (*Frankia*) in non-legumes of the nitrogen-fixing clade, intercellular infection pathways, such as those observed in *Discaria trinervis* (Rhamnaceae) (Imanishi et al. 2011), are the main ones. Intracellular infection via IT is rather exceptional and observed specially in root-hairs of *Casuarina* (Casuarinaceae) (Clavijo et al. 2015). Among legumes, dalbergioid and genistoid, basal Faboideae, do not form IT and rhizobia invade the host roots through breaks in epidermis or wounds where lateral roots emerge (so-called crack entry). The entry modes appear primitive and ancestral compared to the mode via IT that escort rhizobia from epidermis into the cortex (Sprent 2007). In my study, in *L. japonicus*, given that *IAMT1a* was induced by rhizobial infection mainly in epidermis, I initially assumed the involvement of *IAMT1a* in IT formation in epidermis. However, knockdown of *IAMT1a* did not affect IT formation. In addition, a dalbergioid legume *Arachis ipaensis*, which is one of the diploid ancestors of peanut (*Arachis hypogaea*) (Bertioli et al. 2016), and a genistoid legume *Lupinus angustifolius* also possess *IAMT1* gene each in the *IAMT1a* and *IAMT1b* clades, as well as other legumes. Based on these results, it appears that a gene duplication of *IAMT1* and acquisition of *IAMT1a* are not directly related to the acquisition of epidermal IT formation. Given that *IAMT1a* is induced mainly in epidermis but its function was required in cortical events, it is assumed that *IAMT1a* is positioned in signaling to induce cortical development derived from infected epidermis, and could contribute to the coordination between epidermis and cortex during nodulation.

If a model is true that after divergence of dalbergioid and genistoid within Faboideae the others later acquired root-hair infection with IT (Sprent 2007), a gene duplication event of *IAMT1* would have occurred prior to the acquisition of the epidermal infection system; then I can speculate the possibilities that acquisition of *IAMT1a* by a gene duplication of *IAMT1* may have contributed to the establishment of an epidermis-cortex cooperative system before acquisition of IT formation. This scenario is consistent with my results that *IAMT1a* expression is induced prior to epidermal IT formation during symbiotic process and that *IAMT1a* is also induced in *nin* mutant, deficient in IT formation.

The system of nodule symbiosis is a new avenue for understanding auxin methylation.

In the auxin secondary metabolism, auxin methylation stands as one of four processes: amino acid conjugation, oxidation, glycosylation, and methylation. These reactions are carried out by acyl amidosynthetases Gretchen Hagen 3s (GH3s) (Staswick et al. 2005), DIOXYGENASE FOR AUXIN OXIDATION 1/2 (DAO1/2) (Porco et al. 2016; Zhang et al. 2016; Zhao et al. 2013), UDP-Glucosyl transferase 84B1 (UGT84B1) (Aoi et al. 2020; Jackson et al. 2001), and IAMT1 (Abbas et al. 2018; Takubo et al. 2020; Zubieta et al. 2003), respectively. Amino acid conjugation and subsequent oxidation have been shown to be critical for auxin homeostasis (Fukui et al. 2022; Hayashi et al. 2021). Regarding glycosylation, *A. thaliana ugt84b1* mutant has decreased endogenous IAA-Glucose and increased IAA (Aoi et al. 2020), suggesting that glycosylation is also involved in the regulation of auxin homeostasis, although its role remains unclear as no phenotypic changes were observed. Unlike these secondary metabolisms, as for methylation, *iamt1* mutant does not decrease auxin levels and MeIAA is characterized by

extremely low amounts compared to other auxin secondary metabolites (Abbas et al. 2018). Another feature is that although application of other auxin secondary metabolites does not show auxin phenotype, application of MeIAA inhibits elongation of hypocotyl and root and more strongly than IAA when administered at the same concentration (Qin et al. 2005). In this context, administered MeIAA would be demethylated and then affects plant growth, because plants with a null mutation in *AtMES17*, a MeIAA esterase gene, exhibits reduced sensitivity to MeIAA and its overexpression enhances the sensitivity (Yang et al. 2008). Exogenous MeIAA rescues a part of phenotype of Arabidopsis *aux1* mutant (Li et al. 2008), giving an insight that MeIAA can work differently from IAA in terms of physical properties, and auxin methylation may have a biological role in providing IAA with those additional properties. Given that MeIAA is a nonpolar molecule unlike auxin and other auxin conjugates, MeIAA may be able to penetrate cell membrane or move into cells via an AUX1-independent influx system, in which it may act as a donor of IAA.

My study shows that auxin methylation is essential for nodule formation in roots of a leguminous plant *L. japonicus*. This study is also the first example of capturing the increases in endogenous MeIAA in a biological process: Since MeIAA is extremely low in amount, it is difficult to detect quantitative changes in endogenous MeIAA, but the use of *daphne* allowed me to detect for the first time, a significant increase of MeIAA levels associated with induction of *IAMT1a* expression mediated by rhizobial infection. In this manner, the nodule symbiosis system is a new avenue for understanding auxin methylation. The results of induction of *NIN* expression by treatment with MeIAA rather than IAA implicates that auxin methylation is at least not simply an auxin inactivation process. Future functional analysis of *MES17* during the symbiosis process will provide

new insights into the molecular function of MeIAA.

Recently, non-canonical auxin signaling has again received attention: the cell surface auxin receptor ABP1 and its interactor, a transmembrane kinase TMK1, serve ultrafast phosphorylation of a large number of targets including H^+-ATPase, and are responsible for apoplastic acidification, cell required for expansion (Friml et al. 2022; Lin et al. 2021). While MeIAA is not likely to be recognized by a canonical auxin receptor TIR1 (Abbas et al. 2018), association between MeIAA and ABP1/TMK is unknown. Future studies on various possibilities for function of *IAMT1a* and MeIAA in nodule symbiosis are expected to advance study of the establishment of nodule symbiosis as well as signaling of the auxin secondary metabolisms.

ACKNOWLEDGEMENTS

I express my sincere thanks to Prof. Dr. Masayoshi Kawaguchi for his great supervision. Despite my inexperience, he welcomed me into his laboratory and patiently provided me long-term guidance. Although a brilliant and extremely busy scientist, he was very tolerant of my failures and gave me many chances. While allowing me to conduct my research freely, he always watched me from a distance. I feel so lucky to have had the opportunity to work with him and to learn the essence of basic biology.

I would like to thank Dr. Takashi Soyano, Dr. Kensuke Kawade, Dr. Mitsutaka Fukudome, Dr. Nao Okuma, and Dr. Naoki Minamino for their critical suggestion and technical advice; Dr. Meng Liu and Ms. Tomoko Mori for collaboration. Without their guidance, my dissertation would not have been possible. This work was also supported by the following facilities: Functional Genomics Facility (NIBB Core Research Facilities), the Data Integration and Analysis Facility (NIBB), Spectrography and Bioimaging Facility (NIBB Core Research Facilities).

I would like to thank the Life Science Progress Committee, Dr. Takashi Ueda, Dr. Shuji Shigenobu, Dr. Hironori Fujita, Dr. Shoji Mano, Dr. Atsushi Hoshino, and Dr. Yuriko Komine. Discussions with these outstanding scientists are special to my life.

Outside of work, my thanks go to Mr. Sho Hachinoda. He taught me the attractive about Okazaki. Although I experienced so many troubles during my student life, I could enjoy daily life. I am proud of the best friend.

I would like to offer my special thanks to the current and former lab members for their support. Finally, I want to thank my family.

REFERENCES

Abbas, Mohamad, Jorge Hernández-García, Stephan Pollmann, Sophia L. Samodelov, Martina Kolb, Jiří Friml, Ulrich Z. Hammes, Matias D. Zurbriggen, Miguel A. Blázquez, and David Alabadí. 2018. "Auxin Methylation Is Required for Differential Growth in Arabidopsis." *Proceedings of the National Academy of Sciences* 115(26):6864–69. doi: 10.1073/pnas.1806565115.

Akamatsu, Akira, Miwa Nagae, Yuka Nishimura, Daniela Romero Montero, Satsuki Ninomiya, Mikiko Kojima, Yumiko Takebayashi, Hitoshi Sakakibara, Masayoshi Kawaguchi, and Naoya Takeda. 2021. "Endogenous Gibberellins Affect Root Nodule Symbiosis via Transcriptional Regulation of NODULE INCEPTION in Lotus Japonicus." *The Plant Journal* 105(6):1507–20. doi: https://doi.org/10.1111/tpj.15128.

Akamatsu, Akira, Miwa Nagae, and Naoya Takeda. 2022. "The CYCLOPS Response Element in the NIN Promoter Is Important but Not Essential for Infection Thread Formation During Lotus Japonicus–Rhizobia Symbiosis." *Molecular Plant-Microbe Interactions®* 35(8):650–58. doi: 10.1094/MPMI-10-21-0252-R.

Ané, Jean-Michel, György B. Kiss, Brendan K. Riely, R. Varma Penmetsa, Giles E. D. Oldroyd, Céline Ayax, Julien Lévy, Frédéric Debellé, Jong-Min Baek, Peter Kalo, Charles Rosenberg, Bruce A. Roe, Sharon R. Long, Jean Dénarié, and Douglas R. Cook. 2004. "Medicago Truncatula DMI1 Required for Bacterial and Fungal Symbioses in Legumes." *Science* 303(5662):1364 – 1367. doi: 10.1126/science.1092986.

Aoi, Yuki, Hayao Hira, Yuya Hayakawa, Hongquan Liu, Kosuke Fukui, Xinhua Dai, Keita Tanaka, Ken-ichiro Hayashi, Yunde Zhao, and Hiroyuki Kasahara. 2020.

"UDP-Glucosyltransferase UGT84B1 Regulates the Levels of Indole-3-Acetic Acid and Phenylacetic Acid in Arabidopsis." *Biochemical and Biophysical Research Communications* 532(2):244–50. doi: https://doi.org/10.1016/j.bbrc.2020.08.026.

Benson, D. R., and W. B. Silvester. 1993. "Biology of Frankia Strains, Actinomycete Symbionts of Actinorhizal Plants." *Microbiological Reviews* 57(2):293–319. doi: 10.1128/mr.57.2.293-319.1993.

Bertioli, David John, Steven B. Cannon, Lutz Froenicke, Guodong Huang, Andrew D. Farmer, Ethalinda K. S. Cannon, Xin Liu, Dongying Gao, Josh Clevenger, Sudhansu Dash, Longhui Ren, Márcio C. Moretzsohn, Kenta Shirasawa, Wei Huang, Bruna Vidigal, Brian Abernathy, Ye Chu, Chad E. Niederhuth, Pooja Umale, Ana Cláudia G. Araújo, Alexander Kozik, Kyung Do Kim, Mark D. Burow, Rajeev K. Varshney, Xingjun Wang, Xinyou Zhang, Noelle Barkley, Patrícia M. Guimarães, Sachiko Isobe, Baozhu Guo, Boshou Liao, H. Thomas Stalker, Robert J. Schmitz, Brian E. Scheffler, Soraya C. M. Leal-Bertioli, Xu Xun, Scott A. Jackson, Richard Michelmore, and Peggy Ozias-Akins. 2016. "The Genome Sequences of Arachis Duranensis and Arachis Ipaensis, the Diploid Ancestors of Cultivated Peanut." *Nature Genetics* 48(4):438–46. doi: 10.1038/ng.3517.

Breakspear, Andrew, Chengwu Liu, Sonali Roy, Nicola Stacey, Christian Rogers, Martin Trick, Giulia Morieri, Kirankumar S. Mysore, Jiangqi Wen, Giles E. D. Oldroyd, J. Allan Downie, and Jeremy D. Murray. 2014. "The Root Hair 'Infectome' of Medicago Truncatula Uncovers Changes in Cell Cycle Genes and Reveals a Requirement for Auxin Signaling in Rhizobial Infection." *The Plant Cell*

26(12):4680 – 4701. doi: 10.1105/tpc.114.133496.

Broghammer, Angelique, Lene Krusell, Mickaël Blaise, Jørgen Sauer, John T. Sullivan, Nicolai Maolanon, Maria Vinther, Andrea Lorentzen, Esben B. Madsen, Knud J. Jensen, Peter Roepstorff, Søren Thirup, Clive W. Ronson, Mikkel B. Thygesen, and Jens Stougaard. 2012. "Legume Receptors Perceive the Rhizobial Lipochitin Oligosaccharide Signal Molecules by Direct Binding." *Proceedings of the National Academy of Sciences* 109(34):13859–64. doi: 10.1073/pnas.1205171109.

Broughton, W. J., and M. J. Dilworth. 1971. "Control of Leghaemoglobin Synthesis in Snake Beans." *Biochemical Journal* 125(4):1075–80. doi: 10.1042/bj1251075.

Bustos-Sanmamed, Pilar, Guohong Mao, Ying Deng, Morgane Elouet, Ghazanfar Abbas Khan, Jérémie Bazin, Marie Turner, Senthil Subramanian, Oliver Yu, Martin Crespi, and Christine Lelandais-Brière. 2013. "Overexpression of MiR160 Affects Root Growth and Nitrogen-Fixing Nodule Number in *Medicago Truncatula*." *Functional Plant Biology* 40(12):1208–20.

Capella-Gutiérrez, Salvador, José M. Silla-Martínez, and Toni Gabaldón. 2009. "TrimAl: A Tool for Automated Alignment Trimming in Large-Scale Phylogenetic Analyses." *Bioinformatics* 25(15):1972–73. doi: 10.1093/bioinformatics/btp348.

Cerri, Marion R., Lisa Frances, Tom Laloum, Marie-Christine Auriac, Andreas Niebel, Giles E. D. Oldroyd, David G. Barker, Joëlle Fournier, and Fernanda de Carvalho-Niebel. 2012. "Medicago Truncatula ERN Transcription Factors: Regulatory Interplay with NSP1/NSP2 GRAS Factors and Expression Dynamics throughout Rhizobial Infection ." *Plant Physiology* 160(4):2155–72. doi: 10.1104/pp.112.203190.

Cerri, Marion R., Quanhui Wang, Paul Stolz, Jessica Folgmann, Lisa Frances, Katja

Katzer, Xiaolin Li, Anne B. Heckmann, Trevor L. Wang, J. Allan Downie, Andreas Klingl, Fernanda de Carvalho-Niebel, Fang Xie, and Martin Parniske. 2017. “The ERN1 Transcription Factor Gene Is a Target of the CCaMK/CYCLOPS Complex and Controls Rhizobial Infection in Lotus Japonicus.” *New Phytologist* 215(1):323–37. doi: 10.1111/nph.14547.

Clavijo, Fernando, Issa Diedhiou, Virginie Vaissayre, Laurent Brottier, Jennifer Acolatse, Daniel Moukouanga, Amandine Crabos, Florence Auguy, Claudine Franche, Hassen Gherbi, Antony Champion, Valerie Hocher, David Barker, Didier Bogusz, Louis S. Tisa, and Sergio Svistoonoff. 2015. “The Casuarina NIN Gene Is Transcriptionally Activated throughout Frankia Root Infection as Well as in Response to Bacterial Diffusible Signals.” *New Phytologist* 208(3):887–903. doi: https://doi.org/10.1111/nph.13506.

D’Auria, John C., Feng Chen, and Eran Pichersky. 2003. “Chapter Eleven The SABATH Family of MTS in Arabidopsis Thaliana and Other Plant Species.” Pp. 253–83 in *Integrative Phytochemistry: from Ethnobotany to Molecular Ecology*. Vol. 37, edited by J. T. B. T.-R. A. in P. Romeo. Elsevier.

Doebley, John, and Lewis Lukens. 1998. “Transcriptional Regulators and the Evolution of Plant Form.” *The Plant Cell* 10(7):1075–82. doi: 10.1105/tpc.10.7.1075.

Doyle, Jeff J. 2011. “Phylogenetic Perspectives on the Origins of Nodulation.” *Molecular Plant-Microbe Interactions*® 24(11):1289–95. doi: 10.1094/MPMI-05-11-0114.

Ehrhardt, David W., Rebecca Wais, and Sharon R. Long. 1996. “Calcium Spiking in Plant Root Hairs Responding to Rhizobium Nodulation Signals.” *Cell* 85(5):673–81. doi: https://doi.org/10.1016/S0092-8674(00)81234-9.

Emms, David M., and Steven Kelly. 2015. “OrthoFinder: Solving Fundamental Biases in Whole Genome Comparisons Dramatically Improves Orthogroup Inference Accuracy.” *Genome Biology* 16(1):157. doi: 10.1186/s13059-015-0721-2.

Fournier, Joëlle, Alice Teillet, Mireille Chabaud, Sergey Ivanov, Andrea Genre, Erik Limpens, Fernanda de Carvalho-Niebel, and David G. Barker. 2015. “Remodeling of the Infection Chamber before Infection Thread Formation Reveals a Two-Step Mechanism for Rhizobial Entry into the Host Legume Root Hair.” *Plant Physiology* 167(4):1233–42. doi: 10.1104/pp.114.253302.

Friml, Jiří, Michelle Gallei, Zuzana Gelová, Alexander Johnson, Ewa Mazur, Aline Monzer, Lesia Rodriguez, Mark Roosjen, Inge Verstraeten, Branka D. Živanović, Minxia Zou, Lukáš Fiedler, Caterina Giannini, Peter Grones, Mónika Hrtyan, Walter A. Kaufmann, Andre Kuhn, Madhumitha Narasimhan, Marek Randuch, Nikola Rýdza, Koji Takahashi, Shutang Tan, Anastasia Teplova, Toshinori Kinoshita, Dolf Weijers, and Hana Rakusová. 2022. “ABP1–TMK Auxin Perception for Global Phosphorylation and Auxin Canalization.” *Nature* 609(7927):575–81. doi: 10.1038/s41586-022-05187-x.

Fukui, Kosuke, Kazushi Arai, Yuka Tanaka, Yuki Aoi, Vandna Kukshal, Joseph M. Jez, Martin F. Kubes, Richard Napier, Yunde Zhao, Hiroyuki Kasahara, and Ken-ichiro Hayashi. 2022. “Chemical Inhibition of the Auxin Inactivation Pathway Uncovers the Roles of Metabolic Turnover in Auxin Homeostasis.” *Proceedings of the National Academy of Sciences* 119(32):e2206869119. doi: 10.1073/pnas.2206869119.

Gaudioso-Pedraza, Rocio, Martina Beck, Lisa Frances, Philip Kirk, Carolina Ripodas, Andreas Niebel, Giles E. D. Oldroyd, Yoselin Benitez-Alfonso, and Fernanda de

Carvalho-Niebel. 2018. “Callose-Regulated Symplastic Communication Coordinates Symbiotic Root Nodule Development.” *Current Biology* 28(22):3562-3577.e6. doi: https://doi.org/10.1016/j.cub.2018.09.031.

Gonzalez-Rizzo, Silvina, Martin Crespi, and Florian Frugier. 2006. “The Medicago Truncatula CRE1 Cytokinin Receptor Regulates Lateral Root Development and Early Symbiotic Interaction with Sinorhizobium Meliloti.” *The Plant Cell* 18(10):2680–93. doi: 10.1105/tpc.106.043778.

Griesmann, Maximilian, Yue Chang, Xin Liu, Yue Song, Georg Haberer, Matthew B. Crook, Benjamin Billault-Penneteau, Dominique Lauressergues, Jean Keller, Leandro Imanishi, Yuda Purwana Roswanjaya, Wouter Kohlen, Petar Pujic, Kai Battenberg, Nicole Alloisio, Yuhu Liang, Henk Hilhorst, Marco G. Salgado, Valerie Hocher, Hassen Gherbi, Sergio Svistoonoff, Jeff J. Doyle, Shixu He, Yan Xu, Shanyun Xu, Jing Qu, Qiang Gao, Xiaodong Fang, Yuan Fu, Philippe Normand, Alison M. Berry, Luis G. Wall, Jean-Michel Ané, Katharina Pawlowski, Xun Xu, Huanming Yang, Manuel Spannagl, Klaus F. X. Mayer, Gane Ka-Shu Wong, Martin Parniske, Pierre-Marc Delaux, and Shifeng Cheng. 2018. “Phylogenomics Reveals Multiple Losses of Nitrogen-Fixing Root Nodule Symbiosis.” *Science* 361(6398):eaat1743. doi: 10.1126/science.aat1743.

Hayashi, Ken-ichiro, Kazushi Arai, Yuki Aoi, Yuka Tanaka, Hayao Hira, Ruipan Guo, Yun Hu, Chennan Ge, Yunde Zhao, Hiroyuki Kasahara, and Kosuke Fukui. 2021. “The Main Oxidative Inactivation Pathway of the Plant Hormone Auxin.” *Nature Communications* 12(1):6752. doi: 10.1038/s41467-021-27020-1.

Hayashi, Masaki, Akira Miyahara, Shusei Sato, Tomohiko Kato, Makoto Yoshikawa, Michiko Taketa, Makoto Hayashi, Andrea Pedrosa, Ryutaku Onda, Haruko

Imaizumi-Anraku, Andreas Bachmair, Niels Sanda, Jens Stougaard, Yoshikatsu Murooka, Satoshi Tabata, Shinji Kawasaki, Masayoshi Kawaguchi, and Kyuya Harada. 2001. “Construction of a Genetic Linkage Map of the Model Legume Lotus Japonicus Using an Intraspecific F2 Population .” *DNA Research* 8(6):301–10. doi: 10.1093/dnares/8.6.301.

Hayashi, Teruyuki, Yoshikazu Shimoda, Shusei Sato, Satoshi Tabata, Haruko Imaizumi-Anraku, and Makoto Hayashi. 2014. “Rhizobial Infection Does Not Require Cortical Expression of Upstream Common Symbiosis Genes Responsible for the Induction of Ca2+ Spiking.” *The Plant Journal* 77(1):146–59. doi: https://doi.org/10.1111/tpj.12374.

Heckmann, Anne Birgitte, Niels Sandal, Anita Søndergaard Bek, Lene Heegaard Madsen, Anna Jurkiewicz, Mette Wibroe Nielsen, Leila Tirichine, and Jens Stougaard. 2011. “Cytokinin Induction of Root Nodule Primordia in Lotus Japonicus Is Regulated by a Mechanism Operating in the Root Cortex.” *Molecular Plant-Microbe Interactions*® 24(11):1385–95. doi: 10.1094/MPMI-05-11-0142.

Held, Mark, Hongwei Hou, Mandana Miri, Christian Huynh, Loretta Ross, Md Shakhawat Hossain, Shusei Sato, Satoshi Tabata, Jillian Perry, Trevor L. Wang, and Krzysztof Szczyglowski. 2014. “Lotus Japonicus Cytokinin Receptors Work Partially Redundantly to Mediate Nodule Formation.” *The Plant Cell* 26(2):678 – 694. doi: 10.1105/tpc.113.119362.

Hurst, Laurence D., Csaba Pál, and Martin J. Lercher. 2004. “The Evolutionary Dynamics of Eukaryotic Gene Order.” *Nature Reviews Genetics* 5(4):299–310. doi: 10.1038/nrg1319.

Imaizumi-Anraku, Haruko, Naoya Takeda, Myriam Charpentier, Jillian Perry, Hiroki

Miwa, Yosuke Umehara, Hiroshi Kouchi, Yasuhiro Murakami, Lonneke Mulder, Kate Vickers, Jodie Pike, J. Allan Downie, Trevor Wang, Shusei Sato, Erika Asamizu, Satoshi Tabata, Makoto Yoshikawa, Yoshikatsu Murooka, Guo-Jiang Wu, Masayoshi Kawaguchi, Shinji Kawasaki, Martin Parniske, and Makoto Hayashi. 2005. "Plastid Proteins Crucial for Symbiotic Fungal and Bacterial Entry into Plant Roots." *Nature* 433(7025):527–31. doi: 10.1038/nature03237.

Imanishi, Leandro, Alice Vayssières, Claudine Franche, Didier Bogusz, Luis Wall, and Sergio Svistoonoff. 2011. "Transformed Hairy Roots of Discaria Trinervis: A Valuable Tool for Studying Actinorhizal Symbiosis in the Context of Intercellular Infection." *Molecular Plant-Microbe Interactions®* 24(11):1317–24. doi: 10.1094/MPMI-03-11-0078.

Jackson, Rosamond G., Eng-Kiat Lim, Yi Li, Mariusz Kowalczyk, Göran Sandberg, Jim Hoggett, David A. Ashford, and Dianna J. Bowles. 2001. "Identification and Biochemical Characterization of AnArabidopsis Indole-3-Acetic Acid Glucosyltransferase*." *Journal of Biological Chemistry* 276(6):4350–56. doi: https://doi.org/10.1074/jbc.M006185200.

Kalyaanamoorthy, Subha, Bui Quang Minh, Thomas K. F. Wong, Arndt von Haeseler, and Lars S. Jermiin. 2017. "ModelFinder: Fast Model Selection for Accurate Phylogenetic Estimates." *Nature Methods* 14(6):587–89. doi: 10.1038/nmeth.4285.

Kanamori, Norihito, Lene Heegaard Madsen, Simona Radutoiu, Mirela Frantescu, Esben M. H. Quistgaard, Hiroki Miwa, J. Allan Downie, Euan K. James, Hubert H. Felle, Line Lindegaard Haaning, Torben Heick Jensen, Shusei Sato, Yasukazu Nakamura, Satoshi Tabata, Niels Sandal, and Jens Stougaard. 2006. "A Nucleoporin Is Required for Induction of Ca2+ Spiking in Legume Nodule

Development and Essential for Rhizobial and Fungal Symbiosis." *Proceedings of the National Academy of Sciences of the United States of America* 103(2):359 – 364. doi: 10.1073/pnas.0508883103.

Kawaguchi, Masayoshi. 2000. "Lotus Japonicus `Miyakojima' MG-20: An Early-Flowering Accession Suitable for Indoor Handling." *Journal of Plant Research* 113(4):507–9. doi: 10.1007/PL00013961.

Kawaguchi, Masayoshi, Haruko Imaizumi-Anraku, Shungo Fukai, and Kunihiko Syono. 1996. "Unusual Branching in the Seedlings of Lotus Japonicus—Gibberellins Reveal the Nitrogen-Sensitive Cell Divisions within the Pericycle on Roots." *Plant and Cell Physiology* 37(4):461–70. doi: 10.1093/oxfordjournals.pcp.a028968.

Kawaharada, Yasuyuki, Euan K. James, Simon Kelly, Niels Sandal, and Jens Stougaard. 2017. "The Ethylene Responsive Factor Required for Nodulation 1 (ERN1) Transcription Factor Is Required for Infection-Thread Formation in Lotus Japonicus." *Molecular Plant-Microbe Interactions*® 30(3):194–204. doi: 10.1094/MPMI-11-16-0237-R.

Kramer, Elena M., M. Alejandra Jaramillo, and Verónica S. Di Stilio. 2004. "Patterns of Gene Duplication and Functional Evolution During the Diversification of the AGAMOUS Subfamily of MADS Box Genes in Angiosperms." *Genetics* 166(2):1011–23. doi: 10.1093/genetics/166.2.1011.

Lévy, Julien, Cécile Bres, René Geurts, Boulos Chalhoub, Olga Kulikova, Gérard Duc, Etienne-Pascal Journet, Jean-Michel Ané, Emmanuelle Lauber, Ton Bisseling, Jean Dénarié, Charles Rosenberg, and Frédéric Debellé. 2004. "A Putative Ca2+ and Calmodulin-Dependent Protein Kinase Required for Bacterial and Fungal Symbioses." *Science* 303(5662):1361–64. doi: 10.1126/science.1093038.

Li, Linchuan, Xianhui Hou, Tomohiko Tsuge, Maoyu Ding, Takashi Aoyama, Atsuhiro Oka, Hongya Gu, Yunde Zhao, and Li-Jia Qu. 2008. “The Possible Action Mechanisms of Indole-3-Acetic Acid Methyl Ester in Arabidopsis.” *Plant Cell Reports* 27(3):575–84. doi: 10.1007/s00299-007-0458-9.

Lin, Wenwei, Xiang Zhou, Wenxin Tang, Koji Takahashi, Xue Pan, Jiawei Dai, Hong Ren, Xiaoyue Zhu, Songqin Pan, Haiyan Zheng, William M. Gray, Tongda Xu, Toshinori Kinoshita, and Zhenbiao Yang. 2021. “TMK-Based Cell-Surface Auxin Signalling Activates Cell-Wall Acidification.” *Nature* 599(7884):278–82. doi: 10.1038/s41586-021-03976-4.

Liu, Jieyu, Luuk Rutten, Erik Limpens, Tjitse van der Molen, Robin van Velzen, Rujin Chen, Yuhui Chen, Rene Geurts, Wouter Kohlen, Olga Kulikova, and Ton Bisseling. 2019. “A Remote Cis-Regulatory Region Is Required for NIN Expression in the Pericycle to Initiate Nodule Primordium Formation in Medicago Truncatula.” *The Plant Cell* 31(1):68–83. doi: 10.1105/tpc.18.00478.

Lynch, Michael, and John S. Conery. 2000. “The Evolutionary Fate and Consequences of Duplicate Genes.” *Science* 290(5494):1151–55. doi: 10.1126/science.290.5494.1151.

Madsen, Esben Bjørn, Lene Heegaard Madsen, Simona Radutoiu, Magdalena Olbryt, Magdalena Rakwalska, Krzysztof Szczyglowski, Shusei Sato, Takakazu Kaneko, Satoshi Tabata, Niels Sandal, and Jens Stougaard. 2003. “A Receptor Kinase Gene of the LysM Type Is Involved in Legumeperception of Rhizobial Signals.” *Nature* 425(6958):637–40. doi: 10.1038/nature02045.

Maekawa, Takaki, Makoto Maekawa-Yoshikawa, Naoya Takeda, Haruko Imaizumi-Anraku, Yoshikatsu Murooka, and Makoto Hayashi. 2009. “Gibberellin Controls

the Nodulation Signaling Pathway in Lotus Japonicus." *The Plant Journal* 58(2):183–94. doi: 10.1111/j.1365-313X.2008.03774.x.

Magori, Shimpei, Erika Oka-Kira, Satoshi Shibata, Yosuke Umehara, Hiroshi Kouchi, Yoshihiro Hase, Atsushi Tanaka, Shusei Sato, Satoshi Tabata, and Masayoshi Kawaguchi. 2009. "TOO MUCH LOVE, a Root Regulator Associated with the Long-Distance Control of Nodulation in Lotus Japonicus." *Molecular Plant-Microbe Interactions*® 22(3):259–68. doi: 10.1094/MPMI-22-3-0259.

Marsh, John F., Alexandra Rakocevic, Raka M. Mitra, Lysiane Brocard, Jongho Sun, Alexis Eschstruth, Sharon R. Long, Michael Schultze, Pascal Ratet, and Giles E. D. Oldroyd. 2007. "Medicago Truncatula NIN Is Essential for Rhizobial-Independent Nodule Organogenesis Induced by Autoactive Calcium/Calmodulin-Dependent Protein Kinase." *Plant Physiology* 144(1):324 – 335. doi: 10.1104/pp.106.093021.

Middleton, Patrick H., Júlia Jakab, R. Varma Penmetsa, Colby G. Starker, Jake Doll, Péter Kaló, Radhika Prabhu, John F. Marsh, Raka M. Mitra, Attila Kereszt, Brigitta Dudas, Kathryn VandenBosch, Sharon R. Long, Doug R. Cook, Gyorgy B. Kiss, and Giles E. D. Oldroyd. 2007. "An ERF Transcription Factor in Medicago Truncatula That Is Essential for Nod Factor Signal Transduction." *The Plant Cell* 19(4):1221–34. doi: 10.1105/tpc.106.048264.

Miri, Mandana, Preetam Janakirama, Terry Huebert, Loretta Ross, Tim McDowell, Kathleen Orosz, Katharina Markmann, and Krzysztof Szczyglowski. 2019. "Inside out: Root Cortex-Localized LHK1 Cytokinin Receptor Limits Epidermal Infection of Lotus Japonicus Roots by Mesorhizobium Loti." *New Phytologist* 222(3):1523–37. doi: https://doi.org/10.1111/nph.15683.

Miyazawa, Hikota, Erika Oka-Kira, Naoto Sato, Hirokazu Takahashi, Guo-Jiang Wu, Shusei Sato, Masaki Hayashi, Shigeyuki Betsuyaku, Mikio Nakazono, Satoshi Tabata, Kyuya Harada, Shinichiro Sawa, Hiroo Fukuda, and Masayoshi Kawaguchi. 2010. "The Receptor-like Kinase KLAVIER Mediates Systemic Regulation of Nodulation and Non-Symbiotic Shoot Development in Lotus Japonicus." *Development* 137(24):4317 – 4325. doi: 10.1242/dev.058891.

Murray, Jeremy D., Bogumil J. Karas, Shusei Sato, Satoshi Tabata, Lisa Amyot, and Krzysztof Szczyglowski. 2007. "A Cytokinin Perception Mutant Colonized by Rhizobium in the Absence of Nodule Organogenesis." *Science* 315(5808):101–4. doi: 10.1126/science.1132514.

Nadzieja, Marcin, Simon Kelly, Jens Stougaard, and Dugald Reid. 2018. "Epidermal Auxin Biosynthesis Facilitates Rhizobial Infection in Lotus Japonicus." *The Plant Journal* 95(1):101–11. doi: 10.1111/tpj.13934.

Nguyen, Lam-Tung, Heiko A. Schmidt, Arndt von Haeseler, and Bui Quang Minh. 2015. "IQ-TREE: A Fast and Effective Stochastic Algorithm for Estimating Maximum-Likelihood Phylogenies." *Molecular Biology and Evolution* 32(1):268–74. doi: 10.1093/molbev/msu300.

Nizampatnam, Narasimha Rao, Spencer John Schreier, Suresh Damodaran, Sajag Adhikari, and Senthil Subramanian. 2015. "MicroRNA160 Dictates Stage-Specific Auxin and Cytokinin Sensitivities and Directs Soybean Nodule Development." *The Plant Journal* 84(1):140–53. doi: 10.1111/tpj.12965.

Nueda, María José, Sonia Tarazona, and Ana Conesa. 2014. "Next MaSigPro: Updating MaSigPro Bioconductor Package for RNA-Seq Time Series." *Bioinformatics* 30(18):2598–2602. doi: 10.1093/bioinformatics/btu333.

Pecrix, Yann, S. Evan Staton, Erika Sallet, Christine Lelandais-Brière, Sandra Moreau, Sébastien Carrère, Thomas Blein, Marie-Françoise Jardinaud, David Latrasse, Mohamed Zouine, Margot Zahm, Jonathan Kreplak, Baptiste Mayjonade, Carine Satgé, Magali Perez, Stéphane Cauet, William Marande, Céline Chantry-Darmon, Céline Lopez-Roques, Olivier Bouchez, Aurélie Bérard, Frédéric Debellé, Stéphane Muños, Abdelhafid Bendahmane, Hélène Bergès, Andreas Niebel, Julia Buitink, Florian Frugier, Moussa Benhamed, Martin Crespi, Jérôme Gouzy, and Pascal Gamas. 2018. "Whole-Genome Landscape of Medicago Truncatula Symbiotic Genes." *Nature Plants* 4(12):1017–25. doi: 10.1038/s41477-018-0286-7.

Porco, Silvana, Aleš Pěnčík, Afaf Rashed, Ute Voß, Rubén Casanova-Sáez, Anthony Bishopp, Agata Golebiowska, Rahul Bhosale, Ranjan Swarup, Kamal Swarup, Pavlína Peňáková, Ondřej Novák, Paul Staswick, Peter Hedden, Andrew L. Phillips, Kris Vissenberg, Malcolm J. Bennett, and Karin Ljung. 2016. "Dioxygenase-Encoding AtDAO1 Gene Controls IAA Oxidation and Homeostasis in Arabidopsis." *Proceedings of the National Academy of Sciences* 113(39):11016–21. doi: 10.1073/pnas.1604375113.

Qin, Genji, Hongya Gu, Yunde Zhao, Zhiqiang Ma, Guanglu Shi, Yue Yang, Eran Pichersky, Haodong Chen, Meihua Liu, Zhangliang Chen, and Li-Jia Qu. 2005. "An Indole-3-Acetic Acid Carboxyl Methyltransferase Regulates Arabidopsis Leaf Development." *The Plant Cell* 17(10):2693 – 2704. doi: 10.1105/tpc.105.034959.

Radutoiu, Simona, Lene Heegaard Madsen, Esben Bjørn Madsen, Hubert H. Felle, Yosuke Umehara, Mette Grønlund, Shusei Sato, Yasukazu Nakamura, Satoshi Tabata, Niels Sandal, and Jens Stougaard. 2003. "Plant Recognition of Symbiotic

Bacteria Requires Two LysM Receptor-like Kinases." *Nature* 425(6958):585–92. doi: 10.1038/nature02039.

Saito, Katsuharu, Makoto Yoshikawa, Koji Yano, Hiroki Miwa, Hisaki Uchida, Erika Asamizu, Shusei Sato, Satoshi Tabata, Haruko Imaizumi-Anraku, Yosuke Umehara, Hiroshi Kouchi, Yoshikatsu Murooka, Krzysztof Szczyglowski, J. Allan Downie, Martin Parniske, Makoto Hayashi, and Masayoshi Kawaguchi. 2007. "NUCLEOPORIN85 Is Required for Calcium Spiking, Fungal and Bacterial Symbioses, and Seed Production in Lotus Japonicus." *The Plant Cell* 19(2):610–24. doi: 10.1105/tpc.106.046938.

Sandal, Niels, Thomas Rørby Petersen, Jeremy Murray, Yosuke Umehara, Bogumil Karas, Koji Yano, Hirotaka Kumagai, Makoto Yoshikawa, Katsuharu Saito, Masaki Hayashi, Yasuhiro Murakami, Xinwang Wang, Tsuneo Hakoyama, Haruko Imaizumi-Anraku, Shusei Sato, Tomohiko Kato, Wenli Chen, Md. Shakhawat Hossain, Satoshi Shibata, Trevor L. Wang, Keisuke Yokota, Knud Larsen, Norihito Kanamori, Esben Madsen, Simona Radutoiu, Lene H. Madsen, Talida Gratiela Radu, Lene Krusell, Yasuhiro Ooki, Mari Banba, Marco Betti, Nicolas Rispail, Leif Skøt, Elaine Tuck, Jillian Perry, Satoko Yoshida, Kate Vickers, Jodie Pike, Lonneke Mulder, Myriam Charpentier, Judith Müller, Ryo Ohtomo, Tomoko Kojima, Shotaro Ando, Antonio J. Marquez, Peter M. Gresshoff, Kyuya Harada, Judith Webb, Shingo Hata, Norio Suganuma, Hiroshi Kouchi, Shinji Kawasaki, Satoshi Tabata, Makoto Hayashi, Martin Parniske, Krzysztof Szczyglowski, Masayoshi Kawaguchi, and Jens Stougaard. 2006. "Genetics of Symbiosis in Lotus Japonicus: Recombinant Inbred Lines, Comparative Genetic Maps, and Map Position of 35 Symbiotic Loci." *Molecular Plant-Microbe Interactions*® 19(1):80–

91. doi: 10.1094/MPMI-19-0080.

Schauser, Leif, Andreas Roussis, Jiri Stiller, and Jens Stougaard. 1999. “A Plant Regulator Controlling Development of Symbiotic Root Nodules.” *Nature* 402(6758):191–95. doi: 10.1038/46058.

Schiessl, Katharina, Jodi L. S. Lilley, Tak Lee, Ioannis Tamvakis, Wouter Kohlen, Paul C. Bailey, Aaron Thomas, Jakub Luptak, Karunakaran Ramakrishnan, Matthew D. Carpenter, Kirankumar S. Mysore, Jiangqi Wen, Sebastian Ahnert, Veronica A. Grieneisen, and Giles E. D. Oldroyd. 2019. “NODULE INCEPTION Recruits the Lateral Root Developmental Program for Symbiotic Nodule Organogenesis in Medicago Truncatula.” *Current Biology* 29(21):3657-3668.e5. doi: https://doi.org/10.1016/j.cub.2019.09.005.

Shrestha, Arina, Sihui Zhong, Jasmine Therrien, Terry Huebert, Shusei Sato, Terry Mun, Stig U. Andersen, Jens Stougaard, Agnes Lepage, Andreas Niebel, Loretta Ross, and Krzysztof Szczyglowski. 2020. “Lotus Japonicus Nuclear Factor YA1, a Nodule Emergence Stage-Specific Regulator of Auxin Signalling.” *New Phytologist* n/a(n/a). doi: https://doi.org/10.1111/nph.16950.

Sieberer, Björn J., Mireille Chabaud, Antonius C. Timmers, André Monin, Joëlle Fournier, and David G. Barker. 2009. “A Nuclear-Targeted Cameleon Demonstrates Intranuclear Ca2+ Spiking in Medicago Truncatula Root Hairs in Response to Rhizobial Nodulation Factors.” *Plant Physiology* 151(3):1197–1206. doi: 10.1104/pp.109.142851.

Singh, Sylvia, Katja Katzer, Jayne Lambert, Marion Cerri, and Martin Parniske. 2014. “CYCLOPS, A DNA-Binding Transcriptional Activator, Orchestrates Symbiotic Root Nodule Development.” *Cell Host & Microbe* 15(2):139–52. doi:

https://doi.org/10.1016/j.chom.2014.01.011.

Soltis, D. E., P. S. Soltis, D. R. Morgan, S. M. Swensen, B. C. Mullin, J. M. Dowd, and P. G. Martin. 1995. “Chloroplast Gene Sequence Data Suggest a Single Origin of the Predisposition for Symbiotic Nitrogen Fixation in Angiosperms.” *Proceedings of the National Academy of Sciences* 92(7):2647–51. doi: 10.1073/pnas.92.7.2647.

Soyano, Takashi, Hiroshi Kouchi, Atsuko Hirota, and Makoto Hayashi. 2013. “NODULE INCEPTION Directly Targets NF-Y Subunit Genes to Regulate Essential Processes of Root Nodule Development in Lotus Japonicus.” *PLOS Genetics* 9(3):e1003352.

Soyano, Takashi, Yoshikazu Shimoda, Masayoshi Kawaguchi, and Makoto Hayashi. 2019. “A Shared Gene Drives Lateral Root Development and Root Nodule Symbiosis Pathways in Lotus.” *Science* 366(6468):1021 – 1023. doi: 10.1126/science.aax2153.

Sprent, Janet I. 2007. “Evolving Ideas of Legume Evolution and Diversity: A Taxonomic Perspective on the Occurrence of Nodulation.” *New Phytologist* 174(1):11–25. doi: https://doi.org/10.1111/j.1469-8137.2007.02015.x.

Staswick, Paul E., Bogdan Serban, Martha Rowe, Iskender Tiryaki, Marién T. Maldonado, Mitsa C. Maldonado, and Walter Suza. 2005. “Characterization of an Arabidopsis Enzyme Family That Conjugates Amino Acids to Indole-3-Acetic Acid.” *The Plant Cell* 17(2):616–27. doi: 10.1105/tpc.104.026690.

Suzaki, Takuya, Momoyo Ito, Emiko Yoro, Shusei Sato, Hideki Hirakawa, Naoya Takeda, and Masayoshi Kawaguchi. 2014. “Endoreduplication-Mediated Initiation of Symbiotic Organ Development in Lotus Japonicus.” *Development* 141(12):2441 – 2445. doi: 10.1242/dev.107946.

Suzaki, Takuya, Naoya Takeda, Hanna Nishida, Motomi Hoshino, Momoyo Ito, Fumika Misawa, Yoshihiro Handa, Kenji Miura, and Masayoshi Kawaguchi. 2019. "LACK OF SYMBIONT ACCOMMODATION Controls Intracellular Symbiont Accommodation in Root Nodule and Arbuscular Mycorrhizal Symbiosis in Lotus Japonicus." *PLOS Genetics* 15(1):e1007865.

Suzaki, Takuya, Koji Yano, Momoyo Ito, Yosuke Umehara, Norio Suganuma, and Masayoshi Kawaguchi. 2012. "Positive and Negative Regulation of Cortical Cell Division during Root Nodule Development in Lotus Japonicus Is Accompanied by Auxin Response." *Development* 139(21):3997–4006. doi: 10.1242/dev.084079.

Takahara, Masahiro, Shimpei Magori, Takashi Soyano, Satoru Okamoto, Chie Yoshida, Koji Yano, Shusei Sato, Satoshi Tabata, Katsushi Yamaguchi, Shuji Shigenobu, Naoya Takeda, Takuya Suzaki, and Masayoshi Kawaguchi. 2013. "TOO MUCH LOVE, a Novel Kelch Repeat-Containing F-Box Protein, Functions in the Long-Distance Regulation of the Legume–Rhizobium Symbiosis." *Plant and Cell Physiology* 54(4):433–47. doi: 10.1093/pcp/pct022.

Takubo, Eiko, Makoto Kobayashi, Shoko Hirai, Yuki Aoi, Chennan Ge, Xinhua Dai, Kosuke Fukui, Ken-ichiro Hayashi, Yunde Zhao, and Hiroyuki Kasahara. 2020. "Role of Arabidopsis INDOLE-3-ACETIC ACID CARBOXYL METHYLTRANSFERASE 1 in Auxin Metabolism." *Biochemical and Biophysical Research Communications* 527(4):1033–38. doi: https://doi.org/10.1016/j.bbrc.2020.05.031.

Tan, Xu, Luz Irina A. Calderon-Villalobos, Michal Sharon, Changxue Zheng, Carol V Robinson, Mark Estelle, and Ning Zheng. 2007. "Mechanism of Auxin Perception by the TIR1 Ubiquitin Ligase." *Nature* 446(7136):640–45. doi:

10.1038/nature05731.

Tirichine, Leïla, Haruko Imaizumi-Anraku, Satoko Yoshida, Yasuhiro Murakami, Lene H. Madsen, Hiroki Miwa, Tomomi Nakagawa, Niels Sandal, Anita S. Albrektsen, Masayoshi Kawaguchi, Allan Downie, Shusei Sato, Satoshi Tabata, Hiroshi Kouchi, Martin Parniske, Shinji Kawasaki, and Jens Stougaard. 2006. "Deregulation of a Ca2+/Calmodulin-Dependent Kinase Leads to Spontaneous Nodule Development." *Nature* 441(7097):1153–56. doi: 10.1038/nature04862.

Tirichine, Leïla, Niels Sandal, Lene H. Madsen, Simona Radutoiu, Anita S. Albrektsen, Shusei Sato, Erika Asamizu, Satoshi Tabata, and Jens Stougaard. 2007. "A Gain-of-Function Mutation in a Cytokinin Receptor Triggers Spontaneous Root Nodule Organogenesis." *Science* 315(5808):104–7. doi: 10.1126/science.1132397.

Wang, Youning, Wei Yang, Yanyan Zuo, Lin Zhu, April H. Hastwell, Liang Chen, Yinping Tian, Chao Su, Brett J. Ferguson, and Xia Li. 2019. "GmYUC2a Mediates Auxin Biosynthesis during Root Development and Nodulation in Soybean." *Journal of Experimental Botany* 70(12):3165–76. doi: 10.1093/jxb/erz144.

Werner, Gijsbert D. A., William K. Cornwell, Janet I. Sprent, Jens Kattge, and E. Toby Kiers. 2014. "A Single Evolutionary Innovation Drives the Deep Evolution of Symbiotic N2-Fixation in Angiosperms." *Nature Communications* 5(1):4087. doi: 10.1038/ncomms5087.

Yang, Yue, Richard Xu, Choong-je Ma, A. Corina Vlot, Daniel F. Klessig, and Eran Pichersky. 2008. "Inactive Methyl Indole-3-Acetic Acid Ester Can Be Hydrolyzed and Activated by Several Esterases Belonging to the AtMES Esterase Family of Arabidopsis." *Plant Physiology* 147(3):1034 – 1045. doi: 10.1104/pp.108.118224.

Yano, Koji, Seishiro Aoki, Meng Liu, Yosuke Umehara, Norio Suganuma, Wataru

Iwasaki, Shusei Sato, Takashi Soyano, Hiroshi Kouchi, and Masayoshi Kawaguchi. 2017. “Function and Evolution of a Lotus Japonicus AP2/ERF Family Transcription Factor That Is Required for Development of Infection Threads.” *DNA Research* 24(2):193–203. doi: 10.1093/dnares/dsw052.

Yano, Koji, Satoko Yoshida, Judith Müller, Sylvia Singh, Mari Banba, Kate Vickers, Katharina Markmann, Catharine White, Bettina Schuller, Shusei Sato, Erika Asamizu, Satoshi Tabata, Yoshikatsu Murooka, Jillian Perry, Trevor L. Wang, Masayoshi Kawaguchi, Haruko Imaizumi-Anraku, Makoto Hayashi, and Martin Parniske. 2008. “CYCLOPS, a Mediator of Symbiotic Intracellular Accommodation.” *Proceedings of the National Academy of Sciences* 105(51):20540 – 20545. doi: 10.1073/pnas.0806858105.

Yoro, Emiko, Takuya Suzaki, and Masayoshi Kawaguchi. 2019. “CLE-HAR1 Systemic Signaling and NIN-Mediated Local Signaling Suppress the Increased Rhizobial Infection in the Daphne Mutant of Lotus Japonicus.” *Molecular Plant-Microbe Interactions*® 33(2):320–27. doi: 10.1094/MPMI-08-19-0223-R.

Yoro, Emiko, Takuya Suzaki, Koichi Toyokura, Hikota Miyazawa, Hidehiro Fukaki, and Masayoshi Kawaguchi. 2014. “A Positive Regulator of Nodule Organogenesis, NODULE INCEPTION, Acts as a Negative Regulator of Rhizobial Infection in Lotus Japonicus.” *Plant Physiology* 165(2):747–58. doi: 10.1104/pp.113.233379.

Zhang, Jun, Jinshan Ella Lin, Chinchu Harris, Fernanda Campos Mastrotti Pereira, Fan Wu, Joshua J. Blakeslee, and Wendy Ann Peer. 2016. “DAO1 Catalyzes Temporal and Tissue-Specific Oxidative Inactivation of Auxin in Arabidopsis Thaliana.” *Proceedings of the National Academy of Sciences* 113(39):11010–15. doi: 10.1073/pnas.1604769113.

Zhao, Nan, Jean-Luc Ferrer, Jeannine Ross, Ju Guan, Yue Yang, Eran Pichersky, Joseph P. Noel, and Feng Chen. 2008. “Structural, Biochemical, and Phylogenetic Analyses Suggest That Indole-3-Acetic Acid Methyltransferase Is an Evolutionarily Ancient Member of the SABATH Family.” *Plant Physiology* 146(2):455–67. doi: 10.1104/pp.107.110049.

Zhao, Zhigang, Yunhui Zhang, Xi Liu, Xin Zhang, Shichang Liu, Xiaowen Yu, Yulong Ren, Xiaomin Zheng, Kunneng Zhou, Ling Jiang, Xiuping Guo, Ying Gai, Chuanyin Wu, Huqu Zhai, Haiyang Wang, and Jianmin Wan. 2013. “A Role for a Dioxygenase in Auxin Metabolism and Reproductive Development in Rice.” *Developmental Cell* 27(1):113–22. doi: https://doi.org/10.1016/j.devcel.2013.09.005.

Zubieta, Chloe, Jeannine R. Ross, Paul Koscheski, Yue Yang, Eran Pichersky, and Joseph P. Noel. 2003. “Structural Basis for Substrate Recognition in the Salicylic Acid Carboxyl Methyltransferase Family.” *The Plant Cell* 15(8):1704–16. doi: 10.1105/tpc.014548.